bioRxiv preprint doi: https://doi.org/10.1101/097063; this version posted December 29, 2016. The copyright holder for this preprint (which was not certified by peer review) is the author/funder, who has granted bioRxiv a license to display the preprint in perpetuity. It is made available under aCC-BY-NC-ND 4.0 International license.

Metagenomic Characteristics of Bacterial Response to Petroleum Hydrocarbon Contamination in Diverse Environments as Revealed by Functional Taxonomic Strategies

Arghya Mukherjee[1], Bobby Chettri[2], James S. Langpoklakpam[2], Pijush Basak[3@], Aravind Prasad[4‡], Ashis K. Mukherjee[5], Maitree Bhattacharyya[3], Arvind K. Singh[2] and Dhrubajyoti Chattopadhyay[1#*]

[1] Department of Biotechnology, University of Calcutta, Kolkata, West Bengal, India

[2] Department of Biochemistry, North-Eastern Hill University, Shillong, India.

[3] Department of Biochemistry, University of Calcutta, Kolkata, West Bengal, India.

[4] Bioinformatics Resources and Applications Facility, Centre for Development of Advance Computing, Pune, India.

[5] Department of Molecular Biology and Biotechnology, Tezpur University, Tezpur, India

[@] Present address: Jagadis Bose National Science Talent Search, Kolkata, West Bengal, India

[‡] Present address: Institute of Molecular and Cell Biology, A*STAR, Singapore, Singapore

* Present address: Department of Biotechnology, Amity University, Rajarhat, New Town, Kolkata, West Bengal, India

[#] Correspondence and request for materials should be addressed to Dhrubajyoti Chattopadhyay (email: dchattopadhyay@kol.amity.edu).

Abstract

Microbial remediation of oil polluted habitats remains one of the foremost methods for restoration of petroleum hydrocarbon contaminated environments. The development of effective bioremediation strategies however, require an extensive understanding of the

bioRxiv preprint doi: https://doi.org/10.1101/097063; this version posted December 29, 2016. The copyright holder for this preprint (which was not certified by peer review) is the author/funder, who has granted bioRxiv a license to display the preprint in perpetuity. It is made available under aCC-BY-NC-ND 4.0 International license.

resident microbiome of these habitats. Recent developments such as high-throughput sequencing has greatly facilitated the advancement of microbial ecological studies in oil polluted habitats. However, effective interpretation of biological characteristics from these large datasets remains a considerable challenge. In this study, we have implemented recently developed bioinformatic tools for analyzing 65 publicly available 16S rRNA datasets from 12 diverse hydrocarbon polluted habitats to decipher metagenomic characteristics of bacterial communities of the same. We have comprehensively described phylogenetic and functional compositions of these habitats and additionally inferred a multitude of metagenomic features including 255 taxa and 414 functional modules which can be used as biomarkers for effective distinction between the 12 oil polluted sites. We have identified essential metabolic signatures and also showed that significantly over-represented taxa often contribute to either or both, hydrocarbon degradation and additional important functions. Our findings reveal significant differences between hydrocarbon contaminated sites and establishes the importance of endemic factors in addition to petroleum hydrocarbons as driving factors for sculpting hydrocarbon contaminated bacteriomes.

bioRxiv preprint doi: https://doi.org/10.1101/097063; this version posted December 29, 2016. The copyright holder for this preprint (which was not certified by peer review) is the author/funder, who has granted bioRxiv a license to display the preprint in perpetuity. It is made available under aCC-BY-NC-ND 4.0 International license.

Introduction

Anthropogenic activities and agents leading to contamination of the environment is one of the major issues that developing and developed industrial societies face today**.** Petroleum hydrocarbons are the most widespread of these anthropogenic agents and frequently contaminate aquatic and terrestrial ecosystems through releases of hydrocarbon during production, operational use, and transportation. The development, effectiveness and availability of technologies and strategies pose a significant challenge for the remediation, rehabilitation and restoration of these contaminated environments. Many of the technologies developed and in use for the restoration of oil contaminated environments exploit the potential of biological systems, in particular microbial systems, to use these toxic compounds as substrates for growth. Hence, much of the research conducted on bioremediation has concentrated on the capabilities of a single or couple of microbes exhibiting robust and effective growth using petroleum hydrocarbons. However, in the environment, bioremediation is often a complex process involving co-metabolism, cross-induction, inhibition and non-interaction among microbes [1-3], possibly as petroleum hydrocarbons are a mixture of organic pollutants and therefore are used differently by different microbes. These findings, along with others, established bioremediation as a process mediated by a consortium of microbes rather than a few. Thus, characterization of microbial communities of oil contaminated environments could potentially provide guidelines for effective remediation and restoration of such environments.

Until recently, it was only possible to study a handful of microorganisms of interest isolated from source materials (as blood, soil, water or air), given the restrictions of the composition of culture media which cannot reflect and mimic the dynamic nutrient fluxes of the source environment. Indeed, only 1% of microorganisms were found to be cultivable

bioRxiv preprint doi: https://doi.org/10.1101/097063; this version posted December 29, 2016. The copyright holder for this preprint (which was not certified by peer review) is the author/funder, who has granted bioRxiv a license to display the preprint in perpetuity. It is made available under aCC-BY-NC-ND 4.0 International license.

using a set of media from the highly characterized soil rhizosphere [4]. The advent of high throughput massively-parallel sequencing methods has however, allowed us to investigate the entire complement of organisms inhabiting a certain environment. These next-generation sequencing methods (NGS) include a variety of methods to holistically study any biological system such as amplicon sequencing (for variant identification and phylogenetic surveys), whole genome shotgun sequencing (single organism genome and metagenomes) and RNA-Seq (transcriptomes, metatranscriptomes and identification of non-regular RNAs). These powerful methods have ushered in rapid advances in bioinformatics approaches leading to development of software capable of handling huge amounts of data and offering meaningful biological interpretations of the same. Although a technological breakthrough in modern science, a number of NGS methods as metagenomic and transcriptomic/ metatranscriptomic sequencing are still expensive and hence, most studies on ecological processes on bioremediation report marker surveys as 16S rRNA gene amplicon sequencing when dealing with a large number of samples. Thus, in general, most of these studies concentrated on interpretations from microbial community composition but inferred poorly regarding functional and metabolic properties of the same.

Recently, with the implementation of the Human Microbiome Project (HMP), bioinformatic advancements have been furthered through the development of powerful new computational tools for effective interpretation and visualization of taxonomic and functional composition of microbial communities [5,6]. These tools have obvious applications for the analysis of huge amounts of microbial genomic/amplicon/transcriptomic data collected from other sources such as soil, water and so on. Some particularly interesting computational tools allow to explain the complex mutual interactions and heterogeneity

bioRxiv preprint doi: https://doi.org/10.1101/097063; this version posted December 29, 2016. The copyright holder for this preprint (which was not certified by peer review) is the author/funder, who has granted bioRxiv a license to display the preprint in perpetuity. It is made available under aCC-BY-NC-ND 4.0 International license.

inherent in microbial communities through network-based correlation analyses [7], prediction of metagenomic biomarkers [8] and prediction of metagenomes from 16S rRNA data [9].

It is well understood that depending on the environment, the method of bioremediation will vary. However, essential information required for development of these technologies include the response of microbes to petroleum hydrocarbons and their dynamics with the immediate environment. Unfortunately, despite the large amount of work done on microbial community composition across a myriad of oil contaminated environments, mainly through 16S rRNA amplicon sequencing, no attempt has been made to find differential metagenomic signatures among these studies. In the present study, we have aimed to investigate the taxonomic and functional characteristics of diverse oil contaminated environments using recent bioinformatics tools through an evolving pipeline to process metagenomic data. Due to the current paucity of metagenomic datasets for this kind of study and for the large availability of them, we used 61 publicly available 16S rRNA datasets and 4 from this study as inputs for our analysis. Consequently, metagenomic level characteristics of bacterial composition and metabolic potential were comprehensively deduced for oil contaminated soils in north-east India along with 11 other petroleum hydrocarbon contaminated habitats. We inferred an array of differentially abundant taxonomic and functional features which may be used as biomarkers for successful distinction of different oil contaminated habitats as well as for monitoring of bioremediation efforts in the same. Additionally, we deduced important metabolic pathways for all contaminated environments. Evaluation of correlation between taxa and functional orthologs was also carried out along with estimation of metagenomic contributions to hydrocarbon degradation to detect taxa responsible for critical functions in oil polluted habitats. Furthermore, a network of bacterial interaction patterns was inferred to deduce

bioRxiv preprint doi: https://doi.org/10.1101/097063; this version posted December 29, 2016. The copyright holder for this preprint (which was not certified by peer review) is the author/funder, who has granted bioRxiv a license to display the preprint in perpetuity. It is made available under aCC-BY-NC-ND 4.0 International license.

115 complex co-occurrence and co-exclusion relationships in these environments. We found
116 that phylogenetic and functional composition oil contaminated bacteriomes were
117 significantly different to each other and greatly influenced by immediate environmental
118 factors along with petroleum hydrocarbon contamination. Our investigation provides novel
119 and valuable insights into the differential nature of various oil polluted habitats and
120 hopefully improves upon previous understanding of these environments.
121

122 **Materials and Methods**

123 Ethics statement
124

125 No specific permits were required for the samplings carried out at the fields described in
126 Noonmati or Barhola in Assam, India. The study sites are not privately owned or protected
127 in any terms. Also, the field work did not involve any protected or endangered species.
128

129 Collection of soil samples
130

131 Oil contaminated soil samples were collected from Noonmati Oil Refinery in Guwahati and
132 from oilfields in Barhola, both in Assam, India. Soil samples were collected in triplicate from
133 both sites from the surface (0-10 cm) and beneath (20-40 cm) using sterile equipment. The
134 soil samples were transported to the laboratory on ice within 48-72 hours. In the laboratory,
135 replicates for each sample was mixed and homogenized to uniformity to form four
136 composite samples prior to isolation of soil DNA.
137

138 Extraction of total soil DNA

bioRxiv preprint doi: https://doi.org/10.1101/097063; this version posted December 29, 2016. The copyright holder for this preprint (which was not certified by peer review) is the author/funder, who has granted bioRxiv a license to display the preprint in perpetuity. It is made available under aCC-BY-NC-ND 4.0 International license.

Soil DNA was isolated using the PowerMax Soil DNA Isolation Kit (MoBio Labs, Carlsbad, CA, USA) according to the manufacturer's protocol. Integrity of isolated soil DNA was then checked in a 0.8% agarose gel, while a NanoDrop 2000 Spectrophotometer (Thermo Scientific, Wilmington, DE, USA) was used to obtain qualitative (260:280 and 260:230 ratios) and quantitative estimates.

16S rRNA PCR Amplification and Pyrosequencing

The V1-V3 region of the bacterial 16S rRNA gene was amplified using specially designed fusion primers, consisting of both template derived sequence and a specific sequence as recommended by the "Sequencing Technical Bulletin No. 013-2009" (454 Life Sciences, Branford, CT, USA). The Fusion forward primer (5'-3') consisted of a Roche A adapter (CCATCTCATCCCTGCGTGTCTCCGAC), a key sequence (TCAG), a 10 bp Multiplex Identifier (MID) sequence and a template specific sequence (GAGTTTGATCMTGGCTCAG) derived from the universal 16S rRNA primer 27F [10]. The Fusion reverse primer consisted of a Roche B adapter (CCTATCCCCTGTGTGCCTTGGCAGTC), a key sequence (TCAG) and a template specific sequence (ATTACCGCGGCTGCTGG) derived from the universal 16S rRNA gene primer 541R [11]. V1-V3 region of the 16S rRNA gene was amplified through PCR in a 25 µl reaction mix containing 2.5 µl Fast Start Buffer (10X), 1 µl each of Fusion forward primer (10 µM) and Fusion reverse primer (10 µM), 0.5 µl dNTPs (10 mM), 0.5 µl Fast Start Taq Polymerase (5U/µl Fast Start High Fidelity PCR System, Roche) with the rest made up with water. The PCR was carried out in a Veriti Thermal Cycler (Thermo Scientific, Wilmington, DE, USA) under the following conditions: initial denaturation at 94°C for 3 minutes, followed by 25

bioRxiv preprint doi: https://doi.org/10.1101/097063; this version posted December 29, 2016. The copyright holder for this preprint (which was not certified by peer review) is the author/funder, who has granted bioRxiv a license to display the preprint in perpetuity. It is made available under aCC-BY-NC-ND 4.0 International license.

163 cycles of denaturation at 94 °C for 15 secs, annealing at 58 °C for 45 secs and elongation at
164 72 °C for 1 min, with a final elongation at 72 °C for 10 mins. Thereafter samples were stored
165 at -20 °C, if required.
166
167 Sequence processing and taxonomic analysis of 16S rRNA data
168
169 Raw 16S rRNA sequencing reads were checked for quality using FastQC [12] and subsequently
170 processed using mothur [13], which included trimming of adapters, keys, MIDs and primers
171 from the raw sequences. Sequences were further filtered for quality using the following
172 non-default parameters: maxhomop = 6, maxambig = 0, maxlength = 575, minlength = 200,
173 qwindowaverage = 30, bdiffs = 1, pdiffs = 2, and tdiffs = 2. Filtered high quality sequences
174 were then aligned to the mothur implementation of the SILVA database and trimmed for
175 the alignment region. Chimeric sequences were then removed from the datasets using the
176 mothur implementation of Uchime [14]. Filtered sequences were then taxonomically classified
177 using the May 2013 release of the Greengenes database [15] and contaminating archaeal,
178 eukaryal, mitochondrial and chloroplast sequences or sequences classified as unknown were
179 removed from further analysis. mothur was further used to compute coverage, boneh index
180 (for additional 500 sequences), observed species richness, and alpha diversity metrics
181 through the estimation OTUs at 0.03 level of phylogenetic divergence. OTUs were further
182 classified using the taxonomy file generated in the steps before. Taxonomically classified
183 OTUs were converted to number of sequences and visualized as circular cladograms using
184 the standalone graphical tool GraPhlan v0.95 [16].
185
186 Collection and quality filtering of 16S rRNA datasets from oil contaminated environments

bioRxiv preprint doi: https://doi.org/10.1101/097063; this version posted December 29, 2016. The copyright holder for this preprint (which was not certified by peer review) is the author/funder, who has granted bioRxiv a license to display the preprint in perpetuity. It is made available under aCC-BY-NC-ND 4.0 International license.

Sixty-one 16S rRNA datasets on oil degradation studies from 11 different environments collected from publicly available resources along with four samples from this study were used for the present study (Table 1, Supplementary Table S1). These included four datasets representing upper soil layers of the Tundra biome (Tu), four from subsurface layers of the Tundra biome (Tb), four from the permafrost layers of the Tundra (Tp), nine from surface soil of Chinese oil refineries (C), twelve representing different regions of the arctic biome (A), four from surface soils of Indian oil refineries (I), three from mangroves (M), seven from surficial marine sediments (DWH), seven from oil sands cores (OSC), four from surface waters of oil sands tailings ponds (OSTPu), three from oil sands tailings pond waters at median depth (OSTPm) and four from deep oil sands tailings pond waters (OSTPd). We deliberately kept the taiga and OSTP samples separate even though we expected high amounts of similarity between them in certain aspects when compared to other samples, due to evidence of ample distinctive characteristics in the said samples in their parent studies [17,18]. All the 16S rRNA datasets used can be downloaded through the list of accession numbers provided in Supplementary Table S1. All datasets used in the study presented, were sequenced in either Roche 454, Illumina or ABI Ion Torrent platforms. The 16S rRNA datasets are described in greater detail in Table 1. The downloaded 16S rRNA datasets were checked for quality using FastQC and filtered for high quality sequences in mothur using the following criteria: minimum sequence length of 100 bp, sequences trimmed when average quality drops below 20 in a sliding window of 15 bp, and a maximum of 2 mismatches in the barcode-key-template region of the reads.

Analysis of microbial community structure and composition in 16S rRNA datasets

bioRxiv preprint doi: https://doi.org/10.1101/097063; this version posted December 29, 2016. The copyright holder for this preprint (which was not certified by peer review) is the author/funder, who has granted bioRxiv a license to display the preprint in perpetuity. It is made available under aCC-BY-NC-ND 4.0 International license.

mothur was used to estimate abundances of bacterial taxa in the 16S rRNA datasets as described above. Briefly, all the datasets containing high quality reads were aligned against the mothur implementation of the SILVA 16S rRNA database, followed by removal of chimeric sequences using the mothur implementation of Uchime. Classification of the filtered sequences against the Greengenes database was carried out then, upon which contaminating archaeal, chloroplast, mitochondrial, eukaryal or unknown sequences were removed. Finally, OTUs were predicted from these high quality sequences. OTUs were again mapped to the sequence taxonomy file generated previously in mothur to generate comparative taxonomy data for the datasets. We also assessed the compositional similarity between the soil samples from different sites. For doing this, we compared the pairwise taxonomic abundances from each site against each other and within the datasets as well, using Bray-Curtis measure for estimation of beta diversity [19]. The permutation-based multivariate analysis of variance (PERMANOVA) was used to test the homogeneity of taxonomic dispersion across samples along with concomitant estimation of 2D stress. The resulting Bray-Curtis similarity distance matrix was used as input for ordination of the oil contaminated samples through non-metric multidimensional scaling (NMDS) in PAST v3.11 [20].

Metagenome prediction and metabolic reconstruction of 16S rRNA datasets

Metagenomes were predicted from 16S rRNA data using PICRUSt [9]. OTU data generated in mothur for all 16S rRNA datasets was used to prepare *.biom* files formatted as input for PICRUSt v1.1.0 [9] with the *make.biom* script available in mothur. PICRUSt requires OTU

bioRxiv preprint doi: https://doi.org/10.1101/097063; this version posted December 29, 2016. The copyright holder for this preprint (which was not certified by peer review) is the author/funder, who has granted bioRxiv a license to display the preprint in perpetuity. It is made available under aCC-BY-NC-ND 4.0 International license.

abundances mapped to Greengenes OTU IDs as input for prediction of corresponding metagenomes. PICRUSt databases for 16S rRNA copy number normalization and KEGG ortholog prediction were updated using publicly available information listed in Integrated Microbial Genomes (IMG)[21] as on 4th April, 2016, according to the instructions (default settings) provided in the Genome Prediction Tutorial for PICRUSt (http://picrust.github.io/picrust/tutorials/genome_prediction.html#genome-prediction-tutorial). The update involved the inclusion of 16S rRNA copy number information and KEGG ortholog (KO) annotation data as per KEGG v77.1 [22] for ~34,000 bacterial and archaeal genomes available in IMG. 16S rRNA copy numbers for 16S rRNA datasets were normalized using the *normalize_by_copy_number.py* script. Metagenomes were predicted from the copy number normalized 16S rRNA data in PICRUSt using the *predict_metagenomes.py* script against the updated and PICRUSt-formatted, characterized protein functional database of KEGG Orthology. Contributions of various taxa to different KOs were computed with the script *metagenome_contributions.py* and visualized with the script *plot_metagenome_contributions.R* (https://groups.google.com/forum/#!topic/picrust-users/Hq9_G23J9W4) and ggplot [23] in R (http://www.R-project.org). Predicted metagenomes were then used as inputs in HUMAnN2 [24] to estimate the relative abundances of KEGG Pathways and/or KEGG modules. Based on the KO estimates, relative abundance and coverage of KEGG Pathways was inferred by HUMAnN2. KO information was also used by MinPath [25] to infer coverage and relative abundances of KEGG modules, which are manually defined tight, functional units. KEGG Pathways and KEGG modules (KEGG v77.1) data for HUMAnN2 were updated according to publicly available information in IMG [21] and KEGG [22]. Relative abundances and coverages of KEGG modules were represented through circular cladograms generated through GraPhlan.

bioRxiv preprint doi: https://doi.org/10.1101/097063; this version posted December 29, 2016. The copyright holder for this preprint (which was not certified by peer review) is the author/funder, who has granted bioRxiv a license to display the preprint in perpetuity. It is made available under aCC-BY-NC-ND 4.0 International license.

Identification of metagenomic biomarkers

We furthered our study through detection of taxonomic clades, KEGG orthologs and metabolic modules that are significantly over/under-represented in the individual oil contaminated environments through statistical analyses carried out on the inferred relative abundances. To this end, the procedure of linear discriminant analysis (LDA) effect size was employed through LEfSe v1.0 [8] to identify differentially abundant features that can be used as potential metagenomic biomarkers. For this analysis, the alpha parameter significance threshold for the Krushkal-Wallis (KW) test implemented among classes in LEfSe was set to 0.01 and the logarithmic LDA score cut-off was set to 2.0, due to the relatively small sample size under consideration. All analysis carried out through LEfSe was performed through the Galaxy server [26]. Additionally, to estimate the associations between taxonomic and functional enrichments in each oil polluted environment, we carried out tests of correlation between abundances for KEGG orthologs and taxonomic clades using a non-parametric test of Spearman's rank correlation. Detection of significant relationships, defined as a correlation > 0.7 with a p-value < 0.001 and reaching a Benjamini-Hochberg false discovery rate < 0.01 was carried out through the function *corr.test* implemented in the R package, *psych* [27]. Correlations were only computed for oil polluted sites represented by greater than 6 samples. The resultant correlation network was visualized using the interactive platform, Cytoscape v3.4.0 [28].

Detection of microbial interactions

bioRxiv preprint doi: https://doi.org/10.1101/097063; this version posted December 29, 2016. The copyright holder for this preprint (which was not certified by peer review) is the author/funder, who has granted bioRxiv a license to display the preprint in perpetuity. It is made available under aCC-BY-NC-ND 4.0 International license.

Bacterial interactions in oil contaminated environments was investigated in the present study through non-random bacterial co-occurrence and co-exclusion relationships within individual soil sites. Only polluted sites consisting of more than 4 samples were subjected to deductions of bacterial interactions. mothur implementation of the Sparse Correlations for Compositional data algorithm (SparCC) [7], a tool capable of computing significant correlations from compositional data while correcting for the effects of the same, was used to detect significant co-occurrence and co-exclusion patterns. SparCC was run on absolute count OTU tables generated by mothur for each sample, using the command *sparcc* with default settings except a single non-default parameter of permutations=10,000. OTU associations with an absolute SparCC correlation value above 0.6 with *p*-values < 0.01 were considered statistically significant and incorporated into subsequent network construction. The final network of significant SparCC correlations was built in Cytoscape 3.4.0 [28]. The nodes in the reconstructed networks represent OTUs participating in robust, statistically significant relationships (both positive and negative), which are in turn portrayed by edges i.e. connections between the nodes.

Data Availability

16S rRNA amplicon sequencing data generated in this study were deposited in the NCBI Sequence Read Archive (SRA) under accession numbers SRR3168574-SRR3168577. The amplicon sequence data are bundled under NCBI BioProject number PRJNA306989.

Results

Bacterial community composition of oil polluted sediments in India

bioRxiv preprint doi: https://doi.org/10.1101/097063; this version posted December 29, 2016. The copyright holder for this preprint (which was not certified by peer review) is the author/funder, who has granted bioRxiv a license to display the preprint in perpetuity. It is made available under aCC-BY-NC-ND 4.0 International license.

In the present study, we collected oil contaminated samples from sites subjected to regular pollution events in state owned oil refineries at Guwahati and Barhola in the Indian state of Assam to assess the *in situ* bacterial community composition of the same (Table 1). To our knowledge, except for a metagenomic study on oil pipeline microbial populations by Joshi et al. [29], this is the first study of its kind to be performed in India. To add diversity to our samples, sampling was carried out from both surface and subsurface soils. 16S rRNA amplicon sequencing data generated by pyrosequencing was further analyzed through mothur, which classified the resulting OTUs into 465 phylotypes. This included 11 phyla, 29 orders and 28 families identified at ≥ 0.5% abundance in at least one of the samples (Fig. 1, Supplementary Table S2). Proteobacteria was the most dominant phylum in all the samples with an average relative abundance of ≥ 50% (Fig. 2). The relative abundance of Proteobacteria (70%) was higher in the Barhola subsurface sample as compared to others (Fig. S1). Acidobacteria was almost as abundant as Proteobacteria in the Noonmati samples (~40%) while lower abundance was observed in the Barhola samples (~10%) (Supplementary Fig. S1). Bacteroidetes and Chlorobi exhibited increase in abundance in the Barhola surface sample when compared to others while Actinobacteria and Chloroflexi were seen to be present in low but consistent abundance across all samples (Supplementary Fig. S1). At the family level, bacterial community composition was much more divergent than at the phylum level with some of them more abundant in particular samples. For instance, Acidobacteraceae (33%), Xanthomonadaceae (10%) and Sphingomonadaceae (7.5%) were detected at higher abundances in Noonmati surface than in others while Koribacteraceae (25%) and Rhodocyclaceaea (~7%) were found to be more enriched in Noonmati subsurface (Fig. 1). Additionally, Hydrogenophilaceae (~9%) and Hyphomicrobiaceae (~4%) exhibited

bioRxiv preprint doi: https://doi.org/10.1101/097063; this version posted December 29, 2016. The copyright holder for this preprint (which was not certified by peer review) is the author/funder, who has granted bioRxiv a license to display the preprint in perpetuity. It is made available under aCC-BY-NC-ND 4.0 International license.

increased abundance in Barhola subsurface compared to other samples (Fig. 1). Chitinophagaceaea, Ectothiorhodospiraceae and Ignavibacteraceae were more enriched in the Barhola samples, while Acetobacteraceae was found in greater numbers in the Noonmati samples (Fig. 1). All samples, except Noonmati surface, showed a high abundance of Comamonadaceae whereas Weeksellaceae and Syntrophaceaea seemed to be specific to Barhola surface (Fig. 1). Families as Sinobacteraceae, Microbacteriaceae and Solibacteraceae were found in fairly consistent abundances across samples (Fig. 1). Overall, at the phylum level the bacterial community composition of Noonmati samples was observed to be more homogenous and less influenced by sampling depth than the Barhola samples (Fig. 1, Fig. 2, Supplementary Fig. S1).

General characterization of bacterial community composition in petroleum hydrocarbon polluted habitats

Comprehensive characterization of bacterial community composition in hydrocarbon polluted environments was carried out using 61 publicly available and previously validated/published 16S rRNA amplicon sequencing datasets distributed over 11 different habitats (Table 1, Supplementary Table S1) along with 4 datasets generated in this study. mothur analysis of all datasets led to the identification of 18 phyla, 38 orders and 39 families at ≥ 2% abundance in at least one habitat (Fig. 2A, Fig. 2B). Proteobacteria dominated the bacterial community composition at the phylum level with relative abundances ranging from 20-77% across samples (Fig. 2A). Acidobacteria was detected in large numbers in all samples with notably decreased abundances in OSC, OSTPu, OSTPm and OSTPd samples (Fig. 2A, Supplementary Table S1). Actinobacteria and Chloroflexi were consistently

bioRxiv preprint doi: https://doi.org/10.1101/097063; this version posted December 29, 2016. The copyright holder for this preprint (which was not certified by peer review) is the author/funder, who has granted bioRxiv a license to display the preprint in perpetuity. It is made available under aCC-BY-NC-ND 4.0 International license.

355 identified in all samples with significant increase in A samples, while Bacteroidetes showed
356 higher abundance in DWH and I samples (Fig. 2A, Supplementary Table S1). Similar to our
357 findings, an increase in abundance for the Actinobacteria was reported by Yergeau et al. in
358 diesel contaminated arctic soil biopiles [30]. Additionally, Chlorobi was detected in high
359 abundance only in M and I samples with increased Gemmatimonadetes abundance
360 identified in A, C and M samples (Fig. 2A, Supplementary Table S1). Verrucomicrobia
361 contribution in microbial community composition was higher in DWH, M and C, while
362 abundance of Firmicutes was higher in OSTP samples and Cyanobacteria in C samples as
363 compared to others (Fig. 2A, Supplementary Table S1). Order level clades with higher
364 abundances detected at ≥ 2% abundance in at least one habitat, tended to be more specific
365 to certain samples. For instance, Acidobacterales had a 21% abundance in I, while
366 Burkholderiales had an average abundance of 30% across OSTP samples and Caulobacerales
367 had an abundance of ~19% in taiga samples (Fig. 2B, Supplementary Table S1). Additionally,
368 Xanthomonadales showed high abundance (15-20%) in I and DWH samples and
369 Actinomycetales dominated A samples with an abundance of 24% (Fig. 2B, Supplementary
370 Table S1). In addition, Alteromonadales (15%) was found in increased abundance in DWH
371 samples, Ellin329 (15%) abundance was highly elevated in Taiga upper active layer (Tu), and
372 Burkholderiales (25%), Pseudomonadales (27%), Rhizobiales (22%) were enriched in OSC
373 (Fig. 2B, Supplementary Table S1). Bacterial families detected at ≥ 2% abundance in a
374 habitat also exhibited preferential sequestration to certain samples. While
375 Caulobacteraceae and Sphingomonadaceae were highly enriched in the taiga samples with
376 an average relative abundance of ~19% and ~29%, Comamonadaceae exhibited a highly
377 elevated mean abundance of 30% in the OSTP samples (Supplementary Table S1).
378 Additionally, Comamonadaceae dominated the I samples bacteriome with an abundance of

bioRxiv preprint doi: https://doi.org/10.1101/097063; this version posted December 29, 2016. The copyright holder for this preprint (which was not certified by peer review) is the author/funder, who has granted bioRxiv a license to display the preprint in perpetuity. It is made available under aCC-BY-NC-ND 4.0 International license.

379 15% and contributed 10% of the bacteriome in A samples (Supplementary Table S1). Highly
380 specific increases in relative abundance as compared to other samples included
381 Microbacteriaceae (19%) for A samples, Alteromonadaceae (14%) and Xanthomonadaceae
382 (20%) for DWH samples, and Moraxellaceae (26%) for OSC samples (Supplementary Table
383 S1).
384
385 Similarity in bacterial community structure and detection of taxonomic biomarkers of oil
386 polluted environments
387
388 Bray-Curtis similarity scores were inferred from taxonomic data generated by mothur in
389 PAST v3.11 (Table 2) and consequently reduced to a two-dimensional space using NMDS
390 (Fig. 3) for estimation of structural similarity of bacteriomes from petroleum hydrocarbon
391 polluted environments. PERMANOVA tests carried out in PAST showed that taxonomic
392 composition of bacterial communities in the oil polluted environments were significantly
393 varied (p = 0.05). However, there were three exceptions. The PERMANOVA results
394 demonstrated that the taiga samples and OSTP samples were not significantly different
395 among themselves (p = 0.2-0.9) and that bacteriomes at these sites although separated by
396 depth shared substantial similarity. These observations indicated that unlike large distance
397 spatial separation i.e. geographical isolation, depth or local spatial separation is not a major
398 defining factor for effecting substantial dissimilarity. This is well supported by the Bray-
399 Curtis indices (Table 2) and NMDS plots of the same (Fig. 3) wherein all these samples
400 cluster fairly closely. Additionally, polluted mangrove sediments showed similarity with
401 OSTPm and Tp samples (p = 0.057-0.09). Given the very low p values these may be
402 aberrations and may have occurred due to preferences, assumptions, and thresholds set in

bioRxiv preprint doi: https://doi.org/10.1101/097063; this version posted December 29, 2016. The copyright holder for this preprint (which was not certified by peer review) is the author/funder, who has granted bioRxiv a license to display the preprint in perpetuity. It is made available under aCC-BY-NC-ND 4.0 International license.

403 our analysis pipeline. All habitats showed considerable conservation of taxonomic
404 composition within respective samples as described in Table 2. Among these intra-group
405 interactions, OSC samples were indeed clustered in very close proximity (Fig. 3) and
406 exhibited a Bray-Curtis similarity score of 0.85 ± 0.09, which was the highest among all inter
407 and intra-group comparisons (Table 2). Intra-group comparisons of taiga samples showed
408 lowest similarities (Bray-Curtis similarity score 0.45-0.57 ± 0.15) among all habitats, probably
409 due to sampling of source soil from 4 different regions of the China-Russia crude oil pipeline
410 (Table 1, Table 2). Among the inter group comparisons, lowest similarity was observed
411 among M and Tp samples (Bray-Curtis similarity score 0.31 ± 0.02). Apart from the taiga and
412 OSTP samples, which showed inter-group Bray-Curtis similarity score similar to intra-group
413 scores (Table 2), the highest inter-group similarity score of 0.54 ± 0.05 was seen between
414 the relatively related environments of M and DWH.

415 To further investigate taxonomic apportionment and detect differentially abundant
416 clades in various oil polluted environments, we compared the abundances of clades
417 detected at an abundance of ≥ 0.5% in at least 5 samples, at each taxonomic level (Fig. 4).
418 The consequent taxonomic profile inferred for all samples (from domain to species level)
419 was then used by LEfSe to detect metagenomic biomarkers. In all, LEfSe detected 255
420 differentially abundant taxa including 66 families, 47 genera and 11 species level biomarkers
421 across all habitats (Fig. 4, Supplementary Table S2). The largest number of taxonomic
422 biomarkers were detected for the C samples (68) while the lowest were recorded for both
423 OSTPd and Tu (7). The very low number of detected taxonomic biomarkers for OSTPd and
424 Tu may be a fallout of the comparatively higher bacterial community structure similarity
425 between taiga and OSTP samples than others leading to smaller tally of unique and
426 significantly differential clades. Among the biomarkers detected at the family level, families

bioRxiv preprint doi: https://doi.org/10.1101/097063; this version posted December 29, 2016. The copyright holder for this preprint (which was not certified by peer review) is the author/funder, who has granted bioRxiv a license to display the preprint in perpetuity. It is made available under aCC-BY-NC-ND 4.0 International license.

such as *Acetobacteraceae*, *Rhodospirillaceae*, *Ignavibacteriaceae* and *Chitinophagaceae* were attributed to I samples, *Microbacteriaceae* to A, *Pirellulaceae* and *Planctomycetaceae* to C, *Flavobacteriaceae*, *Rhodobacteraceae*, and *Xanthomonadaceae* to DWH, *Erythrobacteraceae* and *Desulfuromonadaceae* to M, *Rhodocyclaceae* to OSTPd, *Pseudomonadaceae*, *Anaerolinaceae* and *Syntrophaceae* to OSTPm, *Comamonadaceae* and *Geobacteraceae* to OSTPu, *Caulobacteraceae*, *Bradyrhizobiaceae*, and *Hyphomicrobiaceae* to Tb, *Methylobacteriaceae* to OSC, *Thermogemmatisporaceae*, *Alcaligenaceae* and *Sphingomonadaceae* to Tp samples and *Burkholderiaceae*, *Nocardioidaceae*, and *Micrococcaceae* to Tu samples (Fig. 4, Supplementary Table S2). At the genus level, *Phenylobacterium* and *Novosphingobium* were detected as biomarkers for Tp samples, while genera such as *Geobacter*, *Syntrophus*, *Microbacerium*, *Mycobacterium*, *HB2_32_21*, *Candidatus_Koribacter*, *Methylobacterium*, *Caulobacter*, and *Rhodococcus* were attributed as biomarkers for OSTPu, OSTPm, A, C, DWH, I, OSC, Tb, and Tu samples respectively (Fig. 4, Supplementary Table S2). Interestingly, LEfSe detected 19 phylum level biomarkers which indicate that preferential proliferation of bacterial lineages emanating from particular higher level taxa, probably driven by hydrocarbon stress, is possible and may lead to definitive compositional differences between oil polluted habitats. Moreover, candidate phyla such as AC1, WS3 and WS6 were identified as biomarkers for OSTP samples which also underline the uniqueness of these environments (Fig. 4, Supplementary Table S2).

Metabolic characterization and functional biomarkers of oil contaminated environments

For understanding the metabolic potential of oil polluted environments and identifying differentially abundant functional features, metagenomes were predicted by

bioRxiv preprint doi: https://doi.org/10.1101/097063; this version posted December 29, 2016. The copyright holder for this preprint (which was not certified by peer review) is the author/funder, who has granted bioRxiv a license to display the preprint in perpetuity. It is made available under aCC-BY-NC-ND 4.0 International license.

PICRUSt using the 16S rRNA gene amplicon data generated. Predicted proteins were classified as KEGG orthologs (KOs) resulting in the identification of 7020 KOs across all samples. Metabolic reconstruction of metagenomes predicted by PICRUSt was carried out in HUMAnN2, which detected 585 KEGG modules across all samples. Among these functional modules, 19 functional modules were present across all samples at a coverage of >90% and were identified as core modules (Fig. 5, Supplementary Fig. S2, Table 3, Supplementary Table S4). Most of the core modules identified are essential for sustenance of prokaryotic life in the environments, such as translation (M00178), central carbon metabolism (M00149), ATP synthesis (M00153, M00157) and nucleotide and amino acid metabolism (M00005, M00020). Rest of the core modules identified were found to be involved in various kinds of transport systems for cations, nutrients and peptides including iron, phosphate, nickel, and amino acids (M00188, M00222, M00223, M00236, M00237, M00239, M00240, M00250, M00254, M00255, M00256, M00258, M00320) (Fig. 5, Supplementary Fig. S2, Table 3, Supplementary Table S4). This is important since these resources are generally present in limiting quantities in nature and often determine the survival and proliferation of microbes in the environment. Additionally, transport systems for lipopolysaccharide (LPS), a principal component of the gram-negative bacterial cell wall, were also understandably identified as core modules and included KEGG functional modules for export of LPS across both cytoplasmic (M00250) and outer membranes (M00320) (Fig. 5, Supplementary Fig. S2, Table 3, Supplementary Table S4). Furthermore, 56 differently covered functional modules were detected across all oil contaminated samples (Fig. 5, Supplementary Fig. S2, Supplementary Table S4). Among these, five modules were completely covered in only one sample while being absent in all others (Fig. 5, Supplementary Fig. S2, Supplementary Table S4). This included structural complexes for

bioRxiv preprint doi: https://doi.org/10.1101/097063; this version posted December 29, 2016. The copyright holder for this preprint (which was not certified by peer review) is the author/funder, who has granted bioRxiv a license to display the preprint in perpetuity. It is made available under aCC-BY-NC-ND 4.0 International license.

475 Manganese/Iron transport (M00243), bacterial proteasomes (M00342) and putative
476 aldouronate transport (M00603), all of which were completely covered only in the C
477 samples (Fig. 5, Supplementary Fig. S2, Supplementary Table S4). This indicates that bacteria
478 in the C site are better equipped for transport of metallic cations, peptide utilization and
479 uptake of plant derived aldouronates than other sites. Furthermore, the presence of a
480 complete complement of D-Xylose transport system (M00215) in the C site also reaffirms
481 bacterial access to hemicellulosic plant material at this site (Fig. 5, Supplementary Fig. S2,
482 Supplementary Table S4). Additionally, glutamate transport system (M00233) was
483 completely covered at only the A site, and RstB-RstA stress response two component system
484 (M00446) at the OSC site (Fig. 5, Supplementary Fig. S2, Supplementary Table S4). The
485 bacteria at A site, thus are extremely capable of utilizing glutamate for growth, while
486 resident bacteria at OSC are better furnished with stress response mechanisms critical in
487 environmental adaptation and survival.

488 In addition to differently covered functional modules, 414 KEGG modules were
489 detected to be differentially abundant in at least one of the 12 contaminated environments
490 (Fig. 5, Supplementary Fig. S2, Supplementary Table S3). The largest number of differentially
491 abundant modules were attributed to the OSC samples (70) while the least (8) were
492 attributed to the OSTPm samples (Fig. 5, Supplementary Fig. S2, Supplementary Table S3).
493 The detection of a higher number of differentially abundant modules in the OSC samples is
494 possibly due to its highly extreme environment as compared to other samples, leading to
495 sequestration of a large number of convenient functions to optimize the use of available
496 resources and counteract distinct environmental stress conditions. On the contrary, similar
497 to the result for taxonomic biomarkers, the least number of differential functional modules
498 were detected in an OSTP sample (OSTPm), with the penultimate spot being taken by Tu

bioRxiv preprint doi: https://doi.org/10.1101/097063; this version posted December 29, 2016. The copyright holder for this preprint (which was not certified by peer review) is the author/funder, who has granted bioRxiv a license to display the preprint in perpetuity. It is made available under aCC-BY-NC-ND 4.0 International license.

(13). As explained above, this is not surprising since both taiga and OSTP samples share comparatively greater similarity between their habitats leading to an overlap of functional capabilities and hence, fewer unique and over-represented functional modules (Fig. 5, Supplementary Fig. S2, Supplementary Table S3). Most of the modules for metabolism of aromatic hydrocarbons such as xylene degradation (M00537), toluene degradation (M0053), benzoate degradation (M00540 and M00551), salicylate degradation (M00638) and catechol ortho-cleavage (M00568) were also significantly associated with the OSC samples (Fig. 5, Supplementary Fig. S2, Supplementary Table S3). A number of structural complexes implicated in photosynthesis were found to be differentially abundant in C samples which included Photosystems I and II (M00163, M00161), the cytochrome b6f complex (M00162) and NADP(H): Quinone oxidoreductase for chloroplasts and cyanobacteria (M00145) (Fig. 5, Supplementary Fig. S2, Supplementary Table S3). Additionally, a plethora of amino acid biosynthesis modules were detected as functional biomarkers in the taiga samples. For example, three different modules for lysine biosynthesis (M00525-M00527), and one each for threonine, methionine and cysteine biosynthesis (M00018, M00017, M00021) were significantly abundant in Tb samples while modules for valine/isoleucine, phenylalanine, tyrosine, leucine and isoleucine biosynthesis (M00019, M00024, M00026, M00040, M00432, M00535, M00570) were over-represented in Tp samples (Fig. 5, Supplementary Fig. S2, Supplementary Table S3). The taiga samples also exhibited an over-representation for modules involved in the biosynthesis of vitamins and cofactors as heme, pantothenate, ubiquinone, tetrahydrofolate, thiamine and ascorbate (M00127, M00129, M00121, M00119, M00128, M00126) (Fig. 5, Supplementary Fig. S2, Supplementary Table S3).

bioRxiv preprint doi: https://doi.org/10.1101/097063; this version posted December 29, 2016. The copyright holder for this preprint (which was not certified by peer review) is the author/funder, who has granted bioRxiv a license to display the preprint in perpetuity. It is made available under aCC-BY-NC-ND 4.0 International license.

Overall, all the sites were found to harbor a variety of differentially abundant modules dedicated to the transport of saccharide, polyols, peptides, metallic cations, vitamin, amino acid, mineral ions, organic ions, lipid and phosphate underlining the large genetic investment of resident bacteria in the processing of environmental information specific to the said site (Fig. 5, Supplementary Fig. S2, Supplementary Table S3). However, while differentially over-represented transport systems for saccharides, polyols and lipids were almost ubiquitously detected, significantly associated transport systems for other substrates as phosphates, amino acids, peptides and organic ions were restrained to certain sites. This may indicate differential availability of these nutrients resulting in preferential dependence on certain substrates acquired from the environment and also reaffirms the characteristically different nature of the environments under consideration. A large number of differentially abundant biosynthetic pathways for sugars, amino acids and vitamins were also detected along with a great diversity of two component systems catering to a range of functions such as stress and redox response, quorum sensing, chemotaxis and heavy metal tolerance across all sites (Fig. 5, Supplementary Fig. S2, Supplementary Table S3). Additionally, some modules for atypical energy metabolism as denitrification, dissimilatory nitrate reduction and dissimilatory sulfate reduction were also detected to be differentially abundant and may be important biomarkers for the corresponding sites due to their contribution in bacterial respiration (Fig. 5, Supplementary Fig. S2, Supplementary Table S3). Finally, several modules describing microbial resistance to antibiotics and antimicrobial peptides were detected to be over-represented at all sites (Fig. 5, Supplementary Fig. S2, Supplementary Table S3). This is probably due to the method of ancestral state reconstruction used by PICRUSt for genome prediction, that leads to these genes being predicted for consequent metagenomes if input 16S rRNA data includes hits from bacteria

bioRxiv preprint doi: https://doi.org/10.1101/097063; this version posted December 29, 2016. The copyright holder for this preprint (which was not certified by peer review) is the author/funder, who has granted bioRxiv a license to display the preprint in perpetuity. It is made available under aCC-BY-NC-ND 4.0 International license.

546 known to have antimicrobial resistance genes. The possession and even expression of these
547 genes probably will not have a significant selective advantage in environments already
548 undergoing natural selection due to oil pollution.
549
550 Associations between bacterial taxa and metagenomic gene families
551
552 Correlations between bacterial abundance and functions enriched at different sites
553 were evaluated following a statistical strategy similar to the approach described by Segata
554 et al. [31]. The results indicated strong and significant associations between a number
555 taxonomic clades and gene families predicted by PICRUSt (Supplementary Fig. S3). A subset
556 of these significant correlations included strong associations between previously detected
557 taxonomic biomarkers and over-represented KOs for each site, which further confirmed the
558 identified taxonomic biomarkers. For example, photosynthetic structural complex genes
559 *cpeA* (K05376) and *psb28-2* (K08904), found to be differentially abundant in C samples
560 exhibited strong positive association with an over-represented cyanobacterial order,
561 Oscillatoriophycideae (Spearman correlation > 0.7, *P*-value < 0.001) (Supplementary Fig. S3).
562 Additionally, an array of genes related to polycyclic aromatic hydrocarbon degradation such
563 as *nidABD*, *phdFGIEK,* and *phtAαBC* (K11943-48, K18251, K18255-57, K18275) were
564 differentially abundant in A samples and also significantly positively correlated to known
565 polyaromatic hydrocarbon degrader and taxonomic biomarker *Mycobacterium* (Spearman
566 correlation > 0.7, *P*-value < 0.001) [32] (Supplementary Fig. S3). In other observations,
567 *Methylobacterium* showed positive correlation with a number of genes associated with the
568 transport of sugars, saccharides and amino acids such as *ggtB-D* (K10232-34), *cebE-G*
569 (K10240-42), *chvE* (K10546), *gguA-B* (K10547-48), and *gluA-D* (K10005-08) in arctic samples

bioRxiv preprint doi: https://doi.org/10.1101/097063; this version posted December 29, 2016. The copyright holder for this preprint (which was not certified by peer review) is the author/funder, who has granted bioRxiv a license to display the preprint in perpetuity. It is made available under aCC-BY-NC-ND 4.0 International license.

570 (Spearman correlation > 0.7, *P*-value < 0.001) (Supplementary Fig. S3). Hydrocarbon
571 degradation genes like *pcaG* (K00448), *bbsH* (K07546) and *pcaL* (K14727) were significantly
572 correlated to class Actinobacteria in a positive manner in the same samples (Spearman
573 correlation > 0.7, *P*-value < 0.001) (Supplementary Fig. S3). In the DWH sample,
574 Colwelliaceae exhibited positive correlations with both anaerobic C4-dicarboxylate
575 transporter (*dcuB*; K07792) and 2-oxopent-4-enoate/cis-2-oxohex-4-enoate hydratase
576 (*bphH, xylJ, tesE*; K18820), an enzyme implicated in oligosaccharide metabolism (Spearman
577 correlation > 0.7, *P*-value < 0.001) (Supplementary Fig. S3). Additionally, genus *HB2.32.21*,
578 associated positively with a number of genes involved in alginate production (*alg44*,
579 *algJXKFE*; K19291-3, K19295-6, K16081), flagellar synthesis/chemotaxis (*qseC*; K07645) and
580 aminobenzoate metabolism gene regulation (*feaR*; K14063) (Spearman correlation > 0.7, *P*-
581 value < 0.001) (Supplementary Fig. S3). Acidobacteria however, was found to be negatively
582 correlated with the *alkB1-2* gene (K00496) coding for alkane-1-monooxygenase (Spearman
583 correlation < - 0.7, *P*-value < 0.001) (Supplementary Fig. S3). In OSC samples, positive
584 correlations were detected between *Methylobacterium* and genes involved in furfural
585 degradation (*hmfABCDEF*; K16874-80) and benzoate degradation (*aliAB*, *badI*; K04116-17,
586 K07536) (Spearman correlation > 0.7, *P*-value < 0.001) (Supplementary Fig. S3).
587 *Methylobacterium*, although an aerobe [33], has been shown to possess anaerobic benzene
588 degradation genes in the genome annotation for *Methylobacterium extorquens* PA1 in KEGG
589 (http://www.genome.jp/kegg-bin/show_pathway?mex01220). Furthermore, a number of
590 two-component systems (TCS) showed strong positive association with *Acinetobacter* and
591 Enterobacteriaceae. *Acinetobacter* was positively correlated with the enrichment of
592 RstA/RstB stress response TCS (K07639, K07661), while Enterobacteriaceae showed

bioRxiv preprint doi: https://doi.org/10.1101/097063; this version posted December 29, 2016. The copyright holder for this preprint (which was not certified by peer review) is the author/funder, who has granted bioRxiv a license to display the preprint in perpetuity. It is made available under aCC-BY-NC-ND 4.0 International license.

593 affirmative relationships with the aerobic stress response sensor kinase ArcB (K07648) and
594 nitrate/nitrite response regulator NarP (K07685) (Supplementary Fig. S3).
595 To further understand the association of bacterial clades with gene families
596 specifically with respect to hydrocarbon degradation, we categorized all taxa contributing to
597 the abundance of genes known to be involved in hydrocarbon degradation at the family and
598 genus level (Supplementary Fig. S4). The results showed that differences existed between
599 major contributors to the abundance of particular hydrocarbonoclastic genes at different
600 sites. For example, abundance for alkane-1-monooxygenase (K00496) was contributed
601 mainly by Alteromonadaceae in DWH samples, Comammonadaceae in I, Mycobacteriaceae
602 and Nocardiaceae in C, Propionibacteriaceae in OSC, and a mixture of Acetobacteraceae,
603 Mycobacteriaceae, Nocardiaceae and Rhodospirillaceae in the taiga samples
604 (Supplementary Fig. S4). Similarly, for protocatechuate-4,5-dioxygenase (K04100-01),
605 Alteromonadaceae were again the major contributors for DWH samples, Comamonadaceae
606 and Methylobacteriaceae for OSC, Rhodocyclaceae for I, Rhodocyclaceae and
607 Comamonadaceae in OSTP, and Comamonadaceae and Bradyrhizobiaceae for taiga samples
608 (Supplementary Fig. S4). These differences in patterns observed at the family level, were
609 even more stark at higher resolutions i.e. genus level, thus effectively differentiating such
610 metagenomic contributors from site to site. This was best demonstrated for the
611 hydrocarbonoclastic gene catechol-1,2-dioxygenase (K03381), for which Alteromonadaceae
612 was found to be the most dominant contributor in both DWH and M samples (Fig. S4).
613 However, at the genus level, it was seen that while *HB2-32-21* was the dominant effector
614 organism in DWH samples, *Marinobacter* was the largest metagenomic contributor for
615 K03381 in the M samples (Supplementary Fig. S4).
616

bioRxiv preprint doi: https://doi.org/10.1101/097063; this version posted December 29, 2016. The copyright holder for this preprint (which was not certified by peer review) is the author/funder, who has granted bioRxiv a license to display the preprint in perpetuity. It is made available under aCC-BY-NC-ND 4.0 International license.

617 Bacterial interactions in oil polluted environments

618

619 To further understand complex ecological relationships in oil polluted environments,
620 bacterial association networks were deduced from estimated taxonomic profiles. For our
621 study, we concentrated on individual oil polluted habitats, i.e. Arctic, China oil refineries, oil
622 sands core and so on. The resulting bacterial correlation networks, inferred at or above the
623 species level, constituted 186 significant relationships among 115 phylotypes ($P < 0.01$) (Fig.
624 6). Among the associations deduced to be significant, 72.58% were detected to share
625 positive correlations while the rest shared antagonistic relationships. Almost half of the co-
626 occurrence patterns identified (46%) were observed between bacteria of the same phyla
627 while more than three-quarters of all negative correlations (78%) were detected between
628 bacteria belonging to distinct phyla (Fig. 6). Thus, our results from the inferred bacterial
629 correlation networks indicated that, co-occurrence of phylotypes was closely related to
630 sharing of evolutionary lineage. For example, in the OSC habitat, phylotypes belonging to
631 proteobacterial family Oxalobacteraceae shared positive pairwise correlations with
632 Moraxellaceae and Enterobacteriaceae phylotypes, both of which belong to phylum
633 Proteobacteria (Fig. 6). Additionally, similar co-occurrence patterns were observed between
634 phylotypes attributed to families belonging to the order Actinomycetales in the C samples.
635 Positive pairwise associations were observed in C samples between phylotypes from
636 families Micrococcaceae and Nocardioidaceae, Intrasporangiaceae and Mycobacteriaceae
637 with Solirubrobacteraceae, and Gaiellaceae and Geodermatophilaceae with
638 Microbacteriaceae, all of which belong to order Actinomycetales (Fig. 6). Furthermore,
639 genera *Arthrospira* and *Phenylobacterium*, both of which belong to family
640 Caulobacteraceae, co-occurred in the Tu samples (Fig. 6). Conversely, bacteria without

bioRxiv preprint doi: https://doi.org/10.1101/097063; this version posted December 29, 2016. The copyright holder for this preprint (which was not certified by peer review) is the author/funder, who has granted bioRxiv a license to display the preprint in perpetuity. It is made available under aCC-BY-NC-ND 4.0 International license.

641 evolutionary commonalities tended to be negatively correlated. For example, in DWH
642 samples, antagonistic relationships were observed between phylotypes belonging to family
643 Flavobacteriaceae from phylum Bacteroidetes and proteobacterial families
644 Desulfuromonadaceae and Desulfobulbaceae (Fig. 6). Similarly, mutual exclusion was
645 observed between phylotypes belonging to family Weeksellaceae of phylum Bacteroidetes
646 and Xanthomonadaceae of phylum Proteobacteria in I samples. Additionally, negatively
647 correlated associations were observed between phylotypes belonging to genera
648 Pelotomaculum and Thiobacillus in OSTPu samples, the former of which belongs to phylum
649 Firmicutes and the latter to phylum Proteobacteria (Fig. 6).
650
651 **Discussion**
652
653 The advent of next-generation sequencing (NGS) technologies have revolutionized
654 investigative approaches into microbial processes. This has led to re-exploration of well-
655 known microbial processes as the nitrogen cycle [34], methane metabolism [35], sulfur cycle [36],
656 heavy metal remediation and petroleum bioremediation [37] along with examination of exotic
657 and extreme environments such as deep-sea hydrothermal vents [38], cold deserts as
658 Antarctica [39] and remote cave systems [40]. During this time, a large amount of work has been
659 done on the microbiology of hydrocarbon degradation using NGS technologies as well [41].
660 Most of these studies employed 16S rRNA based amplicon sequencing while some used
661 metagenomic shotgun sequencing for their enquiries. Although some of these studies have
662 concentrated on prediction of potential biomarkers for oil pollution in certain environments
663 [42,43], no investigative effort has been undertaken to use the large amounts of data
664 generated in oil pollution studies across the world to review, validate and further these

bioRxiv preprint doi: https://doi.org/10.1101/097063; this version posted December 29, 2016. The copyright holder for this preprint (which was not certified by peer review) is the author/funder, who has granted bioRxiv a license to display the preprint in perpetuity. It is made available under aCC-BY-NC-ND 4.0 International license.

studies. In the present study, we report bacterial diversity in oil contaminated soil collected from north-eastern India and describe taxonomic and functional characteristics of oil polluted environments across the world in order to understand the differences and similarities that exist between them. Additionally, we infer a large number of potential biomarkers, both taxonomic and functional, along with co-occurrence networks, which provide new insights into the process of oil bioremediation including taxa and metabolic pathways critical to survival in different oil polluted ecosystems. To this end, we have used 65 16S rRNA datasets from different studies across the world (Table 1, Supplementary Table S1), including 4 datasets generated in this study, and carried out robust *in-silico* analysis with recently developed bioinformatics tools to compare and contrast the same. The principal features and findings of our study are discussed below.

Taxonomic and functional features of oil contaminated soils in India.

To unravel the bacterial community structure, functional characteristics and complex inter-relationships in oil contaminated environments in India, crude oil polluted samples were collected from two oil refineries in north-east India. 16S rRNA amplicon sequencing analysis of the said samples revealed an overall predominance of the metabolically versatile phylum Proteobacteria (Fig. 2, Supplementary Fig. S1), as has been reported previously in other oil polluted sites [44]. Additionally, phylum Acidobacteria was also detected to be prevalent in these samples and was identified as a biomarker as well (Fig. 2, Supplementary Fig. S1, Fig. 4, Supplementary Table S2). Further identification the acidobacterial genera *Edaphobacter* and *Candidatus_Koribacer* as biomarkers underlines the importance of the acidobacterial lineage in the oil contaminated India soils and also indicates a slightly acidic

bioRxiv preprint doi: https://doi.org/10.1101/097063; this version posted December 29, 2016. The copyright holder for this preprint (which was not certified by peer review) is the author/funder, who has granted bioRxiv a license to display the preprint in perpetuity. It is made available under aCC-BY-NC-ND 4.0 International license.

689 environment (Fig. 4, Supplementary Table S2). *Methylibium petroleiphilum* was also
690 detected as a biomarker and contributed significantly to the hydrocarbon degradation
691 capabilities at these sites (Fig. 4, Supplementary Table S2, Supplementary Fig. S4).
692 *Methylibium petroleiphilum*, an aerobic bacterium, has previously been reported to degrade
693 hydrocarbons as methyl tert-butyl ether [45]. Moreover, anaerobic genera as the sulfate
694 dissimilating *Thiobacillus* and the photoautrophic *Ignavibacteriaceae*, were also identified as
695 biomarkers (Fig. 4, Supplementary Table S2). These observations, along with the detection
696 of differentially abundant KEGG modules as dissimilatory sulfate reduction, sulfate => H2S
697 (M00596) and NarX-NarL (nitrate respiration) two-component regulatory system (M00471;
698 also found to be present with complete coverage) (Supplementary Fig. S2, Supplementary
699 Table S3, Supplementary Table S4) indicate that anaerobic processes and taxa play a major
700 role in the oil contaminated India soils. Simultaneously, the identification of over-
701 represented aerobic pathways such as formaldehyde assimilation, serine pathway (M00346)
702 (Supplementary Fig. S2, Supplementary Table S3) and differentially abundant aerobic taxa as
703 *Methylibium* and Chitinophagaceae (Supplementary Fig. 4, Supplementary Table S2)
704 however indicate that these environments may be predominantly aerobic but partially
705 anaerobic or microaerophilic. Over-representation of Chitinophagaceae in these
706 environments also indicate possible availability of chitin as a carbon source [46]. NMDS
707 ordination of taxonomic profiles and estimation of Bray-Curtis similarity indices for I
708 samples show that they share much more similarity amongst themselves than with other
709 sites (Fig. 3, Table 2). I samples showed highest similarity with A samples, which may be due
710 to the enrichment of Acetobacteraceae and Comamonadaceae in both the sites possibly due
711 to oil contamination (Fig. 3, Table 2). This is well demonstrated in metagenomic
712 contributions of both families to hydrocarbonoclastic genes (Supplementary Fig. S4).

bioRxiv preprint doi: https://doi.org/10.1101/097063; this version posted December 29, 2016. The copyright holder for this preprint (which was not certified by peer review) is the author/funder, who has granted bioRxiv a license to display the preprint in perpetuity. It is made available under aCC-BY-NC-ND 4.0 International license.

713 However, whereas both the families are the consistently major contributors for
714 hydrocarbon degrading genes across all I samples, other families are shown to also
715 contribute hydrocarbonoclastic capabilities to samples in A sites (Supplementary Fig. S4).
716 Furthermore, samples collected from India oil refineries show extensive adaptation to oil
717 pollution as revealed by the detection of KOs for known hydrocarbonoclastic genes such as
718 alkane-1-monooxygenase, protocatechuate-3,4-dioxygenase, catechol-1,2-dioxygenase and
719 protocatechuate-4,5-dioxygenase (Supplementary Table S3, Supplementary Fig. S4) along
720 with over-represented hydrocarbon degradation genes such as homogentisate-1,2-
721 dioxygenase and the toluene monooxygenase system (*tmoABCDEF* / *tbuA1A2BCUV*/
722 *touABCDEF*) (data not shown). Bacterial interaction networks inferred by SparCC show a
723 high proportion of co-exclusion relationships, most of which exist between taxa belonging
724 to different evolutionary lineages (Fig. 6). Competitive interactions were observed between
725 aerobic and anaerobic taxa, which indicates co-existence in relative proximity with
726 competition for resources and furthers our inference of a possibly microaerophilic or
727 partially anaerobic oil polluted environment (Fig. 6). One of only two positive correlations
728 was found to be shared between *Methylibium* and *Parvibaculum*, which may endow
729 *Methylibium* with a competitive edge and facilitate its enrichment in the I samples (Fig. 6).
730
731 Validation of bioinformatic pipeline.
732
733 To our knowledge this is the only study that has congregated existing 16S rRNA NGS
734 data generated during experiments on hydrocarbon pollution in different habitats around
735 the world to deduce possible biomarkers and associated bacterial characteristics and
736 interactions. The bioinformatics pipeline we designed to analyze this data employed

bioRxiv preprint doi: https://doi.org/10.1101/097063; this version posted December 29, 2016. The copyright holder for this preprint (which was not certified by peer review) is the author/funder, who has granted bioRxiv a license to display the preprint in perpetuity. It is made available under aCC-BY-NC-ND 4.0 International license.

737 PICRUSt, which is a recently developed tool that uses 16S rRNA data to predict
738 metagenomes for corresponding samples along with LEfSe which predicts potential
739 biomarkers and HUMAnN2 for metabolic reconstruction of PICRUSt predicted
740 metagenomes. It is to be noted however, that KEGG orthologs and KEGG module databases
741 for PICRUSt and HUMAnN2 were meticulously updated (previously PICRUSt KEGG databases
742 included KOs only up to K15039 and HUMAnN had a KEGG module database represented
743 only up to M00378) to include currently available definitions of KEGG functional modules
744 and represent the metabolic terrain of petroleum hydrocarbon contaminated habitats in
745 totality, especially with respect to hydrocarbon degradation, functional modules for which
746 were absent in the original databases. To confidently interpret and infer our results, we
747 validated our findings in both taxonomic and functional aspects. For example, a complete
748 convergence of conclusion was observed when comparing our inferred taxonomic
749 compositions and biomarkers with the findings of Mason et al. [47] for the marine sediments
750 samples. Our analysis of the marine sediment samples identified a highly dominant
751 Gammaproteobacterial genus, HB2-32-21 (Greengenes OTU ID 248394) belonging to the
752 family Alteromonadaceae (Table S2), which was detected as a taxonomic biomarker (Fig. 4)
753 and also contributed significantly to the abundance of hydrocarbon degradation genes at
754 the site (Supplementary Fig. S4). Additionally, Colwelliaceae and Rhodobacteraceae were
755 also detected as over-represented taxonomic biomarkers at the Macondo oil contaminated
756 DWH sample sites (Fig. 4, Supplementary Table S2) with the latter contributing largely
757 abundance of the alkane degrading enzyme, alkane-1-monooxygenase (Supplementary Fig.
758 S4). All these observations, are extremely consistent with the findings of Mason et al. [47] in
759 the original article and furthers their study providing new insights. Moreover, we found
760 important similarities between conclusions inferred by An et al. [17] and our study, regarding

bioRxiv preprint doi: https://doi.org/10.1101/097063; this version posted December 29, 2016. The copyright holder for this preprint (which was not certified by peer review) is the author/funder, who has granted bioRxiv a license to display the preprint in perpetuity. It is made available under aCC-BY-NC-ND 4.0 International license.

761 the oil sands core datasets. In the original study by An et al. [17], the oil sands core was
762 deduced as an aerobic environment with limited oxygen ingress in specific regions leading
763 to regional anaerobiasis. This theory of intermittent oxygen infusion in sections of the oil
764 sands core was strongly supported by the detection of both aerobic and anaerobic pathways
765 of hydrocarbon degradation in the oil sands core. For example, in the oil sands core samples
766 we detected differentially abundant KEGG modules for aerobic degradation of different
767 hydrocarbons as xylene, benzoate, toluene and cumate including metabolism of
768 corresponding intermediates as salicylate and catechol (M0537-40, M00568, M00638)
769 (Supplementary Fig. S2, Supplementary Table S3) [48] alongside a module implicated in
770 anaerobic degradation of benzoate (M00551) (Supplementary Fig. S2, Supplementary Table
771 S3) [49]. The larger number of aerobic hydrocarbonoclastic modules compared to anaerobic
772 modules therefore further validated our bioinformatic pipeline for consequent
773 interpretation of findings in the present study.
774
775 Metabolic reconstruction of oil polluted metagenomes reveals important functional
776 pathways in petroleum hydrocarbon contaminated habitats.
777
778 In order to understand the functional landscape of each oil polluted environment,
779 metagenomes were predicted by PICRUSt from 16S rRNA data and metabolic modules
780 detected using HUMAnN2. We identified 19 core modules which were present across all
781 habitats with a coverage of > 90%. Most of these are involved in processes central to
782 survival of bacteria in the environment. Furthermore, in order to identify preferential
783 genetic investments among resident bacteria at each habitat differentially abundant KOs
784 and KEGG modules were detected through LEfSe. Consequently, we analyzed over-

bioRxiv preprint doi: https://doi.org/10.1101/097063; this version posted December 29, 2016. The copyright holder for this preprint (which was not certified by peer review) is the author/funder, who has granted bioRxiv a license to display the preprint in perpetuity. It is made available under aCC-BY-NC-ND 4.0 International license.

represented KOs and KEGG modules across all habitats to identify broad metabolic signatures that may be indicative of important areas of genetic expenditure, especially outside hydrocarbon degradation. As a result, we identified a number of differential functional pathways dedicated to transport of certain sugars or lipids, biosynthesis of particular biomolecules, stress response, quorum sensing, metabolism of polysaccharides, assimilation and respiration of sulphur and/or nitrogen compounds besides hydrocarbon degradation, across all sites. For example, a large number of putrescine transport complexes (M00193, M00299, M00300) a transport system for arginine/ornithine (M00235) were detected to be differentially abundant for the DWH samples (Fig. 5, Supplementary Fig. S2, Supplementary Table S3). This sequestration of putrescine transporters along with ornithine, which is readily converted by ornithine decarboxylase to putrescine indicates a significant dependence of marine bacteria at an oil polluted site on putrescine. This can be explained by the crucial role putrescine plays in bacteria as an osmoprotectant [50], and therefore its prevalence in a marine oil polluted environment. Similarly, availability and possible use of carbon sources besides hydrocarbons was apparent in the C samples. The differential presence of a complete complement of D-xylose transport system (M00215) and a putative aldouronate transport system (M00603) along with the over-representation of KEGG module M00014 (Glucuronate pathway), strongly indicated that besides petroleum hydrocarbons, plant wastes maybe available as possible sources of energy for resident soil bacteria at the China oil refineries site (Fig. 5, Supplementary Fig. S2, Supplementary Table S3, Supplementary Table S4). Bacteria are known to extracellularly depolymerize methylglucuronoxylan, a polysaccharide made of xylose that constitutes the hemicellulosic component of terrestrial plants [51] leading to the production of aldouronates and xylooligosaccharides. These compounds are taken up and normally converted intracellularly

bioRxiv preprint doi: https://doi.org/10.1101/097063; this version posted December 29, 2016. The copyright holder for this preprint (which was not certified by peer review) is the author/funder, who has granted bioRxiv a license to display the preprint in perpetuity. It is made available under aCC-BY-NC-ND 4.0 International license.

809 to fermentable xylose, leading to generation of energy along with ethanol. Alternatively, D-
810 xylose can also be directly taken up from the environment. Also, two structural complexes
811 for transport of peptides/oligopeptides (M00239 & M00439) were detected to be
812 differentially abundant in the C samples along with bacterial proteasomes (M00342) (Fig. 5,
813 Supplementary Fig. S2, Supplementary Table S3). This indicates that acquisition of
814 environmental peptides and consequent proteasomal degradation of the same, may be the
815 dominant mechanism for obtaining amino acids for assimilatory purposes in the C samples.
816 Interestingly, the DesK-DesR two-component system, implicated in regulation of the *des*
817 gene coding for a desaturase that helps control the saturation state of membrane lipids at
818 low temperatures [52] was detected to be differentially abundant in the arctic samples (Fig. 5,
819 Supplementary Fig. S2, Supplementary Table S3). Furthermore, the FitF-FitH two component
820 system, responsible for insecticidal toxin regulation [53], was over-represented in the urban
821 site of the Indian oil refinery samples (Fig. 5, Supplementary Fig. S2, Supplementary Table
822 S3). This makes sense, since it has previously been shown that relatively higher amount of
823 heat generation in cities compared to rural areas leads to sequestration of insects in urban
824 areas [54]. Sulfur assimilation in bacteria (M00616) was detected to be differentially abundant
825 in OSC samples along with a number of modules dedicated to transfer of sulfur compounds
826 (M00185, M00234, M00238, M00348, M00435-36) indicating a large genetic investment in
827 scavenging and metabolism of sulfur compounds in this site (Fig. 5, Supplementary Fig. S2,
828 Supplementary Table S3). Differential presence of a transport module for thiamine
829 (M00191), which is required for assimilation of sulfonate compounds, furthers affirms this
830 notion (Fig. 5, Supplementary Fig. S2, Supplementary Table S3). Additionally, differential
831 detection of assimilatory nitrate reduction module (M00531) also indicates the availability
832 and importance of nitrate ions in the sustenance of the OSC bacteriome (Fig. 5,

bioRxiv preprint doi: https://doi.org/10.1101/097063; this version posted December 29, 2016. The copyright holder for this preprint (which was not certified by peer review) is the author/funder, who has granted bioRxiv a license to display the preprint in perpetuity. It is made available under aCC-BY-NC-ND 4.0 International license.

833 Supplementary Fig. S2, Supplementary Table S3). Sulfate and nitrate ions are also important
834 molecules in anaerobic respiration, and may therefore also play crucial roles in bacterial
835 survival in the anaerobic regions of the OSC. Interestingly, reduction of nitrate has been
836 reported to be closely linked to anaerobic degradation of benzene and concomitant growth
837 [55], functional modules for both of which have been differentially detected in OSC samples
838 (Fig. 5, Supplementary Fig. S2, Supplementary Table S3). Unlike other oil polluted sites, a
839 large number of hydrocarbonoclastic modules differentially detected in the OSC samples
840 (see previous section), whereas only two transport systems for small sugars (M00204,
841 M00215) and no major polysaccharide metabolism and/or transport pathways were
842 detected to be over-represented (Fig. 5, Supplementary Fig. S2, Supplementary Table S3).
843 This not only indicates at the extreme habitat with highly restricted availability of carbon
844 sources other than petroleum hydrocarbons in the OSC, it also explains the large clustering
845 of differentially abundant hydrocarbon degradation pathways in the OSC samples and
846 establishes petroleum hydrocarbons as the comprehensively dominant carbon
847 assimilation/energy production source for this site. A number of functional modules related
848 to methane metabolism, both methanogenic and methanotrophic, were detected to be
849 over-represented for the OSTP samples. For example, methanogenesis (M00356) was over-
850 represented in OSTPu, along with methane assimilation modules M00344-45 and M00608
851 detected to be differentially abundant in OSTPu and OSTPm respectively (Fig. 5,
852 Supplementary Fig. S2, Supplementary Table S3). Oil sands tailings ponds are known to be
853 important sources of methanogenesis and of methylotrophy [17], where deeper regions tend
854 to be highly anaerobic. Additionally, modules for copper processing (M00762) and copper
855 tolerance sensor (M00452) were detected in OSTPd (Fig. 5, Supplementary Fig. S2,
856 Supplementary Table S3). This is important, since copper is an essential component of

bioRxiv preprint doi: https://doi.org/10.1101/097063; this version posted December 29, 2016. The copyright holder for this preprint (which was not certified by peer review) is the author/funder, who has granted bioRxiv a license to display the preprint in perpetuity. It is made available under aCC-BY-NC-ND 4.0 International license.

857 particulate methane monooxygenase (pMMO), and its availability can therefore determine
858 the survivability of methanotrophs [56] along with the ratio of soluble and particulate MMO in
859 the environment. A large number of modules dedicated to the biosynthesis of amino acids,
860 vitamins and co-factors were detected to be over-represented in the taiga samples. This
861 may be due to the poor availability of useful forms of amino acids and vitamins in the taiga
862 environment. Presence of differentially abundant modules for sulfur containing amino acid
863 biosynthesis (M00017, M00021) is supported by the detection of over-represented sulfur
864 assimilation modules (M00176, M00595) which involve biosynthesis of cysteine and
865 methionine as final/supplementary steps [57,58] (Fig. 5, Supplementary Fig. S2, Supplementary
866 Table S3). Additionally, presence of alternative carbon sources as pectin and component
867 sugars of other plant polysaccharides at the taiga sites can be inferred through the presence
868 of differentially abundant functional modules for pectin degradation (M00081), and uptake
869 and metabolism of other sugar and sugar derivatives as N-Acetylglucosamine, N, N'-
870 Diacetylchitobiose, D-glucuronate, aldouronates, D-galactouronate (M00606, M00205,
871 M00061, M00603, M00631) (Fig. 5, Supplementary Fig. S2, Supplementary Table S3). In the
872 M samples, two component systems for starvation of phosphate (M00434), a limiting
873 nutrient for mangroves [59] and metal tolerance (M00499) were detected as differentially
874 abundant (Fig. 5, Supplementary Fig. S2, Supplementary Table S3). Genetic investment in
875 metal tolerance should be important in M samples as mangroves in Brazil are routinely
876 subjected to pollution from factory effluents [42]. Furthermore, the clustering of differentially
877 abundant central carbohydrate metabolism pathways (M00001-2, M00004, M00009,
878 M00011) along with transport systems for fructose like sugars (M00273) in M samples,
879 indicate availability of simple sugars as carbon sources besides hydrocarbons (Fig. 5,
880 Supplementary Fig. S2, Supplementary Table S3). This is also supported by the differentially

bioRxiv preprint doi: https://doi.org/10.1101/097063; this version posted December 29, 2016. The copyright holder for this preprint (which was not certified by peer review) is the author/funder, who has granted bioRxiv a license to display the preprint in perpetuity. It is made available under aCC-BY-NC-ND 4.0 International license.

881 abundant module for synthesis of trehalose (M00565), a known carbohydrate energy
882 storage compound and anti-desiccation agent [60], from glucose (Fig. 5, Supplementary Fig.
883 S2, Supplementary Table S3). All functional modules for degradation of aromatic
884 hydrocarbons were detected to be differentially abundant in OSC, DWH, taiga and OSTP (in
885 that order) samples (Fig. 5, Supplementary Fig. S2, Supplementary Table S3). This is probably
886 because these environments tend to be more extreme than other sites described in this
887 study and coupled with oil pollution, the bacterial metabolic pathways in these
888 environments have been further sculpted to rely greatly only on petroleum hydrocarbons
889 for growth. Additionally, sulfate and nitrate utilization modules have been identified in most
890 of these sites, which indicates an abundance of such ions in the environment and therefore
891 use of the same for anaerobic alkane degradation, as previously described [61]. Our results
892 thus indicate that for all habitats, genetic composition of the bacteriome is representative of
893 the immediate environment especially in terms of substrate usage, nutrient availability,
894 energy metabolism, biosynthesis of compounds, and survival strategies including quorum
895 sensing, chemotaxis, and stress response. Our findings reveal pathways differentially
896 important in these oil polluted environments, especially those not related to hydrocarbon
897 degradation and can therefore be used for differentiation between habitats of interest.
898 Further empirical studies will however be required strengthen these observations and
899 pinpoint functional biomarkers absolutely exclusive to oil polluted environments in specific
900 biomes.
901
902 Taxonomic biomarkers make important contributions to hydrocarbonoclastic and additional
903 functional capacities in oil polluted environments.
904

bioRxiv preprint doi: https://doi.org/10.1101/097063; this version posted December 29, 2016. The copyright holder for this preprint (which was not certified by peer review) is the author/funder, who has granted bioRxiv a license to display the preprint in perpetuity. It is made available under aCC-BY-NC-ND 4.0 International license.

In order to identify taxonomic clades that may be differentially abundant in oil polluted sites used in the present study, taxonomic profiles generated through analysis of 16S rRNA data in mothur were examined using LEfSe. Additionally, to decipher functional associations of taxonomic clades, direct correlations between KOs and taxa were determined along with metagenomic contributions to hydrocarbonoclastic genes. Furthermore, bacterial co-occurrence and co-exclusion networks were deduced to understand important bacterial interactions in oil polluted sites. Our findings suggest that, taxonomic biomarkers inferred in our study contribute significantly to important functions in the oil polluted metabolic landscape and are often determined by their oil degradation capabilities. For example, biomarkers for DWH samples *HB2.32.21* and Alteromonadaceae (Fig. 4, Supplementary Table S2), were associated with over-represented KOs implicated in alginate biosynthesis (Supplementary Fig. S3). Moreover, a two component pathway involved in the regulation of alginate production (M00505) was also differentially abundant in DWH samples (Fig. 5, Supplementary Fig. S2, Supplementary Table S3). Interestingly, previous studies have shown that alginates provide increased mechanical stability to bacterial biofilms [62], and can therefore be instrumental in aiding anchorage or adhesion of DWH Alteromonadaceae. *HB.32.21* and Alteromonadaceae were found to be important contributors in hydrocarbonoclastic properties of the DWH bacteriome (Supplementary Fig. S4) and the former also exhibited strong associations with regulation of genes for aminobenzoate metabolism through *feaR* (see Results). Furthermore, another taxonomic biomarker identified for DWH samples, Colwelliaceae, was closely associated to the anaerobic C4-dicarboxylate transporter DcuB, which is responsible for transport of molecules as fumarate, succinate and malate [63]. This is important, as it may help the facultatively aerobic Colwelliaceae to degrade alkanes anaerobically by addition of fumarates in marine

bioRxiv preprint doi: https://doi.org/10.1101/097063; this version posted December 29, 2016. The copyright holder for this preprint (which was not certified by peer review) is the author/funder, who has granted bioRxiv a license to display the preprint in perpetuity. It is made available under aCC-BY-NC-ND 4.0 International license.

929 sediments [61]. Similarly, *Mycobacterium* was detected as a biomarker for C samples (Fig. 4,
930 Supplementary Table S2) and correlated strongly with KOs implicated in degradation of
931 hydrocarbons as naphthalene, benzoate and phthalate (Supplementary Fig. S3).
932 *Mycobacterium* have previously been shown to harbor the ability to degrade a variety of
933 aromatic hydrocarbons such as naphthalene, anthracene, phenanthrene, pyrene and so on
934 [32]. Phylum Cyanobacteria, a biomarker for C samples (Fig. 4, Supplementary Table S2),
935 strongly correlated with differentially abundant photosynthetic proteins *cpeA* (K05376) and
936 *psb28-2* (K08904) through an over-represented cyanobacterial order for C samples,
937 Oscillatoriophycideae (Fig. 4, Supplementary Table S2). Additionally, KEGG modules for
938 photosynthesis such as Photosystems I and II (M00163, M00161), cytochrome b6f complex
939 (M00162) and NADP(H):quinone oxidoreductase for chloroplasts and cyanobacteria
940 (M00145) were also found to be over-represented in C samples (Fig. 5, Supplementary Fig.
941 S2, Supplementary Table S3). These observations indicated important, differential and extra-
942 hydrocarbonoclastic contributions of Cyanobacteria in C samples. Furthermore,
943 *Microbacterium*, which is known to be a stringent chemoorganotroph [64], was identified to
944 be differentially abundant in A samples (Fig. 4, Supplementary Table S2). *Microbacterium*
945 was found to share close associations with KOs involved in over-represented transport
946 systems dedicated to acquisition of organic compounds such as cellobiose (M00206), alpha-
947 glucosides (M00201), glutamate (M00227, M00233) and multiple sugars (M00207, M00216,
948 M00221) (Supplementary Fig. S3), which can be used as possible sources of carbon and
949 energy and also indicates availability of the same in the environment. Phylum
950 Actinobacteria and class Actinobacteria, which were detected as biomarkers in the A
951 samples, exhibited significant correlations with almost all differentially abundant KOs for A
952 samples including hydrocarbon degrading genes as *pcaG*, phenol-2-monooxygenase, *bbsH*,

bioRxiv preprint doi: https://doi.org/10.1101/097063; this version posted December 29, 2016. The copyright holder for this preprint (which was not certified by peer review) is the author/funder, who has granted bioRxiv a license to display the preprint in perpetuity. It is made available under aCC-BY-NC-ND 4.0 International license.

953 and *pcaL* (data not shown). In OSC samples, over-represented taxa *Methylobacterium* was
954 associated with genes involved in degradation of furfural and other hydrocarbons
955 (Supplementary Fig. S3). The presence of the strongly aerobic *Methylobacterium* [33] once
956 again reinforces the finding of ample availability of oxygen in the OSC. Interestingly,
957 differentially abundant taxa Enterobacteriaceae and *Acinetobacter* were detected to be
958 associated with a number of KOs implicated in stress response which included TCS KOs for
959 aerobic/anaerobic survival as ArcB and NarP and transcriptional regulation of the *mar-sox-*
960 *rob* regulon (Supplementary Fig. S3). The *mar-sox-rob* regulon has been reported in
961 coordinating survival against various environmental stresses activated by inducers as
962 paraquat, decanoate and intriguingly, salicylate [65], functional modules for which is
963 differentially abundant in OSC samples (Fig. 5. Supplementary Fig. S2, Supplementary Table
964 S3). Additionally, *Acinetobacter* was correlated with the stress response serine protease
965 DegS and iron starvation Fe/S biogenesis protein NfuA (Supplementary Fig. S3). Thus, these
966 biomarkers seem to contribute to important stress response pathways rather than
967 hydrocarbon degrading capabilities. Additionally, over-represented taxa such as
968 Oxalobacteraceae, *Cupriavidus*, Brucellaceae, and *Ochrobactrum* (Fig. 4, Supplementary
969 Table S2) were found to differentially contribute to the abundance of a number of
970 hydrocarbonoclastic genes (K00446, K00448-51, K03381) (Supplementary Fig. S4) in the OSC
971 samples. In taiga samples, a number of detected biomarkers such as *Phenylobacterium,*
972 Caulobacteraceae, Sphingomonadaceae, *Novosphingobium*, *Rhodococcus,* and
973 Burkholderiaceae (Fig. 4, Supplementary Table S2) were found to contribute heavily but
974 differently to the abundance of a plethora of hydrocarbonoclastic genes (Supplementary
975 Fig. S4). Differentially abundant functional modules for the assimilation of sulphate,
976 transformation of thiosulphate to sulphate and regulation of the SOX complex responsible

bioRxiv preprint doi: https://doi.org/10.1101/097063; this version posted December 29, 2016. The copyright holder for this preprint (which was not certified by peer review) is the author/funder, who has granted bioRxiv a license to display the preprint in perpetuity. It is made available under aCC-BY-NC-ND 4.0 International license.

977 for thiosulphate transformation (M00176, M00595, M00523) underline the preferential
978 sulphur usage in this site (Fig. 5, Supplementary Fig. S2, Supplementary Table S3). This is
979 well supported by the identification of *Bradyrhizobium*, *Caulobacter*, and *Burkholderia* as
980 biomarkers (Fig. 4, Supplementary Table S2), all which are known to be involved in sulfur
981 metabolism [66,67] and house homologous genes for the same. Interestingly, a number of
982 biomarkers identified here for the taiga samples such as *Phenylobacterium,*
983 Sphingomonadaceae, *Novosphingobium* and *Rhodococcus* were detected as "habitat
984 specialists" in oil contaminated taiga samples by Yang et al. [68]. Similar to the results of An et
985 al. [17], we encountered a significantly high proportion of anaerobic taxa in the OSTP samples,
986 among which Anaerolinaceae, Syntrophaceae, Desulfobulbaceae, Peptococcaceae,
987 Geobacteraceae, Syntrophorhabdaceae and the thermophilic Caldiserica [69] were detected
988 as biomarkers (Fig. 4, Supplementary Table S2). Detected taxonomic biomarkers such as
989 Anaerolinaceae and Comamonadaceae (Fig. 4, Supplementary Table S2) were found to
990 make significant contributions to the abundance of hydrocarbon degradation genes
991 (Supplementary Fig. S4) in OSTP samples. Other identified biomarkers such as
992 Geobacteraceae and *Thauera* (Fig. 4, Supplementary Table S2) are well known anaerobic
993 hydrocarbon degraders [70,71]. Additionally, another detected biomarker Nitrospirales (Fig. 4,
994 Supplementary Table S2), which is involved in nitrification [72] may contribute to nitrification,
995 for which over-represented module ammonia => nitrite transformation (M00528) was
996 identified in OSTP samples (Fig. 5, Supplementary Fig. S2, Supplementary Table S3).
997 Biomarkers of sulfate reducing bacteria such as Desulfuromonadales and Desulfobulbaceae
998 (Fig. 4, Supplementary Table S2), which is a known mesophilic/psychrophilic sulfate reducer
999 [73] may be involved in important sulfur metabolism pathways known to be important in
1000 OSTPs [74]. Interestingly, obligate anaerobes Anaerolinaceae have previously been associated

bioRxiv preprint doi: https://doi.org/10.1101/097063; this version posted December 29, 2016. The copyright holder for this preprint (which was not certified by peer review) is the author/funder, who has granted bioRxiv a license to display the preprint in perpetuity. It is made available under aCC-BY-NC-ND 4.0 International license.

with sulfate reducing conditions in the OSTPs [75]. Lastly, major contributions for hydrocarbonoclastic capabilities in OSTP samples was also observed from biomarkers *Pseudomonas* (K00446, K00448, K00449, K00496, K03381) and Rhodocyclaceae (K04100-01) (Fig. 4, Supplementary Table S2, Supplementary Fig. S4), furthering the hydrocarbon degradation capabilities of OSTPs.

We also investigated significant bacterial associations in oil polluted sites to decipher important co-occurrence and co-exclusions. Our results showed that greater co-occurrence exists between phylotypes sharing an evolutionary lineage while more co-exclusions were observed between phylotypes from different ancestries. This observation has also been previously reported in microbial correlation studies in the environment [76,77]. Interestingly, not a large proportion of taxonomic biomarkers were observed to be represented in these significant correlations. This can possibly happen due to separation of niches due to various environmental and even temporal factors. For example, in the bacterial association network for DWH samples, biomarker Colwelliaceae was detected to participate in a significantly positive relationship with Desulfobulbaceae, a strictly anaerobic sulfate utilizing bacterial family (Fig. 6). The existence of this kind of a relationship, based on degradation of recalcitrant hydrocarbons, was inferred upon by the original authors too [47]. Strikingly however, the most abundant and robust hydrocarbon degrader i.e. *HB2.32.21* (Supplementary Fig. S4) was not detected to be involved in any significant associations. This observation can be explained by a possible individual capacity of survival for *HB2.32.21* due to its hydrocarbonoclastic capacities without extensive interactions with other resident bacteria, therefore occupying a separate niche in the oil polluted marine sediment site. Thus, significant correlations (both positive and negative) may be driven by factors other than only oil pollution in oil contaminated sites with apparently benign taxa being involved

bioRxiv preprint doi: https://doi.org/10.1101/097063; this version posted December 29, 2016. The copyright holder for this preprint (which was not certified by peer review) is the author/funder, who has granted bioRxiv a license to display the preprint in perpetuity. It is made available under aCC-BY-NC-ND 4.0 International license.

in such interactions. This indicates that biomarkers and correlation networks must be studied in tandem to deduce meaningful conclusions. Even though empirical evidence in support of the natural presence of most microbial association networks is lacking, our study shows that they may be important to holistic interpretation of results as well as being a good starting point for further investigations.

Our results therefore show that, detected biomarkers may contribute differently to strictly hydrocarbonoclastic properties when compared across sites, but their close association with a majority of differentially abundant KOs and as an extension a number of over-represented functional pathways for each site underlines their significance in these oil contaminated sites. We find that although many of the taxonomic biomarkers contribute to hydrocarbonoclastic capacities, some do not and can therefore contribute to other possibly important functions. These observations not only elucidate important taxa contributing functions more specific and essential to each site, but also shows that niches related to functions other than hydrocarbon degradation may significantly influence bacteriome structure in oil polluted sites, possibly more in sites with understandably lower degrees of contamination. This indicates clearly that while hydrocarbonoclastic capabilities may be a driving force for continued survival in these sites, other immediate factors including availability of different organic and inorganic compounds and environmental stress play heavily on the evolution of the bacteriome. Thus, we see that a combination of oil degradation capabilities and environmental factors shape the landscape for bacterial petroleum degradation. As an extension, it therefore becomes imperative to examine oil bioremediation processes, especially aimed at empirical identification of biomarkers, in totality with due comparison to similar studies and not in isolation as it may lead to misleading conclusions. This is well illustrated in some previous studies that have focused on

bioRxiv preprint doi: https://doi.org/10.1101/097063; this version posted December 29, 2016. The copyright holder for this preprint (which was not certified by peer review) is the author/funder, who has granted bioRxiv a license to display the preprint in perpetuity. It is made available under aCC-BY-NC-ND 4.0 International license.

predicting microbial markers or proxies for oil pollution in certain environments [42,43]. In the study on mangrove oil pollution and detection of microbial proxies by dos Santos et al. [43], *Marinobacter*, belonging to family Alteromonadaceae, was identified as a possible biomarker for oil pollution in mangroves. However, in our study when compared to other sites, Alteromonadaceae was detected to be differentially abundant in the DWH samples and *Marinobacter* was not identified as over-represented in any of the oil polluted sites (Fig. 4, Supplementary Table S2).

Conclusion

In summary, our study showed that significant taxonomic and functional differences exist between geographically and/or spatially isolated oil polluted sites and that oil pollution is not the sole driving factor in determination of the bacteriome at these sites, even if maybe the most predominant one. In our study we have successfully detected functions that are important and contribute significantly to the sustenance of bacteriomes at these oil polluted sites. Additionally, we have detected taxa that are differentially abundant and also contribute to many of these functions. Furthermore, we have also successfully shown that several of these important taxonomic clades and functional modules are often involved in extra-hydrocarbonoclastic activities, thus underlining the importance of these apparently peripheral niches related to endemic environmental responses such as variable resource utilization, alternate respiration and stress response in the survival of oil contaminated ecosystems. In the process, we therefore identified robust taxonomic and functional biomarkers, that are representative of an entire oil polluted environment and not only its hydrocarbonoclastic capabilities. These biomarkers can be implemented in monitoring of

bioRxiv preprint doi: https://doi.org/10.1101/097063; this version posted December 29, 2016. The copyright holder for this preprint (which was not certified by peer review) is the author/funder, who has granted bioRxiv a license to display the preprint in perpetuity. It is made available under aCC-BY-NC-ND 4.0 International license.

bacterial remediation processes as well as for distinguishing one of the 12 oil polluted habitats. Our results show that some parallels exist in the functional composition of oil polluted environments, mainly regarding adaptations to aerobic and anaerobic lifestyles depending on availability of limited resources compatible with sustenance of anaerobic growth (e.g. sulfate/nitrate related metabolism), but differences between them pertaining to transport of substrates, biosynthesis of biomolecules, response to various stress, degradation of diverse compounds and so on are significant and together with differences identified in taxonomic profiles and hydrocarbonoclastic capabilities enable us to truly differentiate between them. However, further studies are required which may involve simultaneous 16S rRNA based phylogenetic survey, metagenomic and metatranscriptomic investigations of oil polluted environments followed by empirical experimentations on the same to confirm robust and significantly differential taxonomic and functional biomarkers which may be used for monitoring. With the current sequencing technologies, bioinformatics tools and increasing data from other studies, it is highly possible that characteristic degradation profiles and subsequent remediation strategies for different environments across the world will be inferred fairly soon with unprecedented confidence. To our knowledge, this is the first population genomics study carried out on petroleum hydrocarbon polluted habitats. Our study presents novel understanding of oil contaminated habitats by showing how and in what manner petroleum hydrocarbons fashion the metagenomic fabric along with the evident effect of endemic factors characteristic of geographically separated diverse petroleum hydrocarbon contaminated environments, while interpreting the effects of both on the resident microbiome. This study therefore provides a foundation for future investigations into the microbial biodiversity and habitat function in oil polluted sites.

bioRxiv preprint doi: https://doi.org/10.1101/097063; this version posted December 29, 2016. The copyright holder for this preprint (which was not certified by peer review) is the author/funder, who has granted bioRxiv a license to display the preprint in perpetuity. It is made available under aCC-BY-NC-ND 4.0 International license.

Acknowledgements

The authors acknowledge the financial support provided for the research presented above from the Department of Biotechnology, Government of India vide Sanction no. BT/306/NE/TBP/2012 dated December 6, 2012, under the DBT-Twinning scheme. A.M. was supported by the CSIR/UGC-NET Fellowship from the University Grants Commission, Government of India (201112-NETJRF-10217-100). We thank the Bioinformatics Resources and Applications Facility (BRAF), CDAC, Pune and the Centre for High Performance Computing for Modern Biology, University of Calcutta for granting access to supercomputing facilities along with their unconditional and continuous help. We would also like to thank the ICZMP, World Bank and Department of Biochemistry, University of Calcutta for allowing us to use the Pyrosequencing facility. Lastly, we would like to acknowledge the DST-Purse, Department of Biotechnology, University of Calcutta and the University of Calcutta for providing the necessary infrastructure for implementation of the research work furnished above.

Author contributions

D.C. and A.K.S. managed the project. A.M., D.C. and A.K.S. conceptualized and designed the experiments. B.C., J.L., A.K.S. and A.K.M. designed and conducted sampling for oil contaminated soil. A.M., B.C., J.L., P.B. and M.B. were involved in designing the sequencing strategy and conducting the same. A.M. designed the bioinformatic analysis strategy and

bioRxiv preprint doi: https://doi.org/10.1101/097063; this version posted December 29, 2016. The copyright holder for this preprint (which was not certified by peer review) is the author/funder, who has granted bioRxiv a license to display the preprint in perpetuity. It is made available under aCC-BY-NC-ND 4.0 International license.

conducted the same with assistance from A.P. A.M. and D.C. performed the data analyses. A.M, D.C. and A.K.S. prepared the manuscript. All authors reviewed the manuscript.

Competing financial interests

The authors declare no competing financial interests.

References

1 Dean-Ross, D., Moody, J. & Cerniglia, C. E. Utilization of mixtures of polycyclic aromatic hydrocarbons by bacteria isolated from contaminated sediment. *FEMS microbiology ecology* **41**, 1-7, doi:10.1111/j.1574-6941.2002.tb00960.x (2002).

2 Molina, M., Araujo, R. & Hodson, R. E. Cross-induction of pyrene and phenanthrene in a Mycobacterium sp. isolated from polycyclic aromatic hydrocarbon contaminated river sediments. *Canadian journal of microbiology* **45**, 520-529 (1999).

3 Stringfellow, W. T. & Aitken, M. D. Competitive metabolism of naphthalene, methylnaphthalenes, and fluorene by phenanthrene-degrading pseudomonads. *Applied and environmental microbiology* **61**, 357-362 (1995).

4 Bakken, L. R. Culturable and non-culturable bacteria in soil. *J.D. van Elsas, J.T. Trevor, E.M.H. Wellington (Eds.), Modern soil microbiology, Marcel Dekker, New York* 47-61 (1997).

5 Gevers, D. *et al.* The Human Microbiome Project: a community resource for the healthy human microbiome. *PLoS biology* **10**, e1001377, doi:10.1371/journal.pbio.1001377 (2012).

6 Segata, N. *et al.* Computational meta'omics for microbial community studies. *Molecular systems biology* **9**, 666, doi:10.1038/msb.2013.22 (2013).

7 Friedman, J. & Alm, E. J. Inferring correlation networks from genomic survey data. *PLoS computational biology* **8**, e1002687, doi:10.1371/journal.pcbi.1002687 (2012).

bioRxiv preprint doi: https://doi.org/10.1101/097063; this version posted December 29, 2016. The copyright holder for this preprint (which was not certified by peer review) is the author/funder, who has granted bioRxiv a license to display the preprint in perpetuity. It is made available under aCC-BY-NC-ND 4.0 International license.

8 Segata, N. *et al.* Metagenomic biomarker discovery and explanation. *Genome biology* **12**, R60, doi:10.1186/gb-2011-12-6-r60 (2011).

9 Langille, M. G. *et al.* Predictive functional profiling of microbial communities using 16S rRNA marker gene sequences. *Nature biotechnology* **31**, 814-821, doi:10.1038/nbt.2676 (2013).

10 Weisburg, W. G., Barns, S. M., Pelletier, D. A. & Lane, D. J. 16S ribosomal DNA amplification for phylogenetic study. *Journal of bacteriology* **173**, 697-703 (1991).

11 Lofgren, J. L. *et al.* Lack of commensal flora in Helicobacter pylori-infected INS-GAS mice reduces gastritis and delays intraepithelial neoplasia. *Gastroenterology* **140**, 210-220, doi:10.1053/j.gastro.2010.09.048 (2011).

12 Andrews, S. FastQC: a quality control tool for high throughput sequence data. *Available online at: http://www.bioinformatics.babraham.ac.uk/projects/fastqc* (2010).

13 Schloss, P. D. *et al.* Introducing mothur: open-source, platform-independent, community-supported software for describing and comparing microbial communities. *Applied and environmental microbiology* **75**, 7537-7541, doi:10.1128/AEM.01541-09 (2009).

14 Edgar, R. C., Haas, B. J., Clemente, J. C., Quince, C. & Knight, R. UCHIME improves sensitivity and speed of chimera detection. *Bioinformatics* **27**, 2194-2200, doi:10.1093/bioinformatics/btr381 (2011).

15 DeSantis, T. Z. *et al.* Greengenes, a chimera-checked 16S rRNA gene database and workbench compatible with ARB. *Applied and environmental microbiology* **72**, 5069-5072, doi:10.1128/AEM.03006-05 (2006).

16 Asnicar, F., Weingart, G., Tickle, T. L., Huttenhower, C. & Segata, N. Compact graphical representation of phylogenetic data and metadata with GraPhlAn. *PeerJ* **3**, e1029, doi:10.7717/peerj.1029 (2015).

17 An, D. *et al.* Metagenomics of hydrocarbon resource environments indicates aerobic taxa and genes to be unexpectedly common. *Environmental science & technology* **47**, 10708-10717, doi:10.1021/es4020184 (2013).

bioRxiv preprint doi: https://doi.org/10.1101/097063; this version posted December 29, 2016. The copyright holder for this preprint (which was not certified by peer review) is the author/funder, who has granted bioRxiv a license to display the preprint in perpetuity. It is made available under aCC-BY-NC-ND 4.0 International license.

1171 18 Yang, S., Wen, X., Zhao, L., Shi, Y. & Jin, H. Crude oil treatment leads to shift of bacterial
1172 communities in soils from the deep active layer and upper permafrost along the China-
1173 Russia Crude Oil Pipeline route. *PloS one* **9**, e96552, doi:10.1371/journal.pone.0096552
1174 (2014).
1175 19 Bray, J. R. & Curtis, J. T. An ordination of the upland forest communities of southern
1176 Wisconsin. *Ecol Monographs* **27**, 325-349 (1957).
1177 20 Hammer, Ø., Harper, D. A. T. & Ryan, P. D. PAST: Paleontological Statistics Software Package
1178 for Education and Data Analysis. *Palaeontologia Electronica* **4**, 9pp (2001).
1179 21 Markowitz, V. M. *et al.* IMG: the Integrated Microbial Genomes database and comparative
1180 analysis system. *Nucleic acids research* **40**, D115-122, doi:10.1093/nar/gkr1044 (2012).
1181 22 Kanehisa, M., Goto, S., Furumichi, M., Tanabe, M. & Hirakawa, M. KEGG for representation
1182 and analysis of molecular networks involving diseases and drugs. *Nucleic acids research* **38**,
1183 D355-360, doi:10.1093/nar/gkp896 (2010).
1184 23 Wickham, H. ggplot2: Elegant Graphics for Data Analysis. *Springer-Verlag New York* (2009).
1185 24 Abubucker, S. *et al.* Metabolic reconstruction for metagenomic data and its application to
1186 the human microbiome. *PLoS computational biology* **8**, e1002358,
1187 doi:10.1371/journal.pcbi.1002358 (2012).
1188 25 Ye, Y. & Doak, T. G. A parsimony approach to biological pathway reconstruction/inference
1189 for genomes and metagenomes. *PLoS computational biology* **5**, e1000465,
1190 doi:10.1371/journal.pcbi.1000465 (2009).
1191 26 Goecks, J., Nekrutenko, A., Taylor, J. & Galaxy, T. Galaxy: a comprehensive approach for
1192 supporting accessible, reproducible, and transparent computational research in the life
1193 sciences. *Genome biology* **11**, R86, doi:10.1186/gb-2010-11-8-r86 (2010).
1194 27 Revelle, W. psych: Procedures for Personality and Psychological Research. (2016).
1195 28 Shannon, P. *et al.* Cytoscape: a software environment for integrated models of biomolecular
1196 interaction networks. *Genome research* **13**, 2498-2504, doi:10.1101/gr.1239303 (2003).

bioRxiv preprint doi: https://doi.org/10.1101/097063; this version posted December 29, 2016. The copyright holder for this preprint (which was not certified by peer review) is the author/funder, who has granted bioRxiv a license to display the preprint in perpetuity. It is made available under aCC-BY-NC-ND 4.0 International license.

1197 29 Joshi, M. N. *et al.* Metagenomic approach for understanding microbial population from
1198 petroleum muck. *Genome announcements* **2**, doi:10.1128/genomeA.00533-14 (2014).
1199 30 Yergeau, E., Sanschagrin, S., Beaumier, D. & Greer, C. W. Metagenomic analysis of the
1200 bioremediation of diesel-contaminated Canadian high arctic soils. *PloS one* **7**, e30058,
1201 doi:10.1371/journal.pone.0030058 (2012).
1202 31 Segata, N. *et al.* Composition of the adult digestive tract bacterial microbiome based on
1203 seven mouth surfaces, tonsils, throat and stool samples. *Genome biology* **13**, R42,
1204 doi:10.1186/gb-2012-13-6-r42 (2012).
1205 32 Kim, S. J., Kweon, O. & Cerniglia, C. E. Degradation of Polycyclic Aromatic Hydrocarbons by
1206 Mycobacterium Strains. *Handbook of Hydrocarbon and Lipid Microbiology*, 1865-1879.
1207 33 Green, P. N. Methylobacterium. *The Prokaryotes: Proteobacteria: Alpha and Beta Subclasses*
1208 **5**, 257-265, doi:10.1007/0-387-30745-1_14 (2006).
1209 34 Jurkowski, A., Reid, A. H. & Labov, J. B. Metagenomics: a call for bringing a new science into
1210 the classroom (while it's still new). *CBE life sciences education* **6**, 260-265 (2007).
1211 35 Guo, J. *et al.* Dissecting microbial community structure and methane-producing pathways of
1212 a full-scale anaerobic reactor digesting activated sludge from wastewater treatment by
1213 metagenomic sequencing. *Microbial cell factories* **14**, 33 (2015).
1214 36 He, Y., Feng, X., Fang, J., Zhang, Y. & Xiao, X. Metagenome and Metatranscriptome Revealed
1215 a Highly Active and Intensive Sulfur Cycle in an Oil-Immersed Hydrothermal Chimney in
1216 Guaymas Basin. *Frontiers in microbiology* **6**, 1236 (2015).
1217 37 Kuppusamy, S. *et al.* Pyrosequencing analysis of bacterial diversity in soils contaminated
1218 long-term with PAHs and heavy metals: Implications to bioremediation. *Journal of hazardous*
1219 *materials* **317**, 169-179 (2016).
1220 38 Cerqueira, T. *et al.* Microbial diversity in deep-sea sediments from the Menez Gwen
1221 hydrothermal vent system of the Mid-Atlantic Ridge. *Marine genomics* **24 Pt 3**, 343-355,
1222 doi:10.1016/j.margen.2015.09.001 (2015).

bioRxiv preprint doi: https://doi.org/10.1101/097063; this version posted December 29, 2016. The copyright holder for this preprint (which was not certified by peer review) is the author/funder, who has granted bioRxiv a license to display the preprint in perpetuity. It is made available under aCC-BY-NC-ND 4.0 International license.

1223 39 Tytgat, B. *et al.* Bacterial diversity assessment in Antarctic terrestrial and aquatic microbial
1224 mats: a comparison between bidirectional pyrosequencing and cultivation. *PloS one* **9**,
1225 e97564, doi:10.1371/journal.pone.0097564 (2014).
1226 40 Barton, H. A. *et al.* Microbial diversity in a Venezuelan orthoquartzite cave is dominated by
1227 the Chloroflexi (Class Ktedonobacterales) and Thaumarchaeota Group I.1c. *Frontiers in*
1228 *microbiology* **5**, 615, doi:10.3389/fmicb.2014.00615 (2014).
1229 41 Mukherjee, A. & Chattopadhyay, D. Exploring environmental systems and processes through
1230 next-generation sequencing technologies: insights into microbial response to petroleum
1231 contamination in key environments. *The Nucleus*, doi:10.1007/s13237-016-0190-3 (2016).
1232 42 Andreote, F. D. *et al.* The microbiome of Brazilian mangrove sediments as revealed by
1233 metagenomics. *PloS one* **7**, e38600, doi:10.1371/journal.pone.0038600 (2012).
1234 43 dos Santos, H. F. *et al.* Mangrove bacterial diversity and the impact of oil contamination
1235 revealed by pyrosequencing: bacterial proxies for oil pollution. *PloS one* **6**, e16943,
1236 doi:10.1371/journal.pone.0016943 (2011).
1237 44 Hernandez-Raquet, G. *et al.* Molecular diversity studies of bacterial communities of oil
1238 polluted microbial mats from the Etang de Berre (France). *FEMS microbiology ecology* **58**,
1239 550-562, doi:10.1111/j.1574-6941.2006.00187.x (2006).
1240 45 Kane, S. R. *et al.* Whole-genome analysis of the methyl tert-butyl ether-degrading beta-
1241 proteobacterium Methylibium petroleiphilum PM1. *Journal of bacteriology* **189**, 1931-1945,
1242 doi:10.1128/JB.01259-06 (2007).
1243 46 Rosenberg, E. The Family Chitinophagaceae. *The Prokaryotes: Other Major Lineages of*
1244 *Bacteria and The Archaea*, 493-495, doi:10.1007/978-3-642-38954-2_137 (2014).
1245 47 Mason, O. U. *et al.* Metagenomics reveals sediment microbial community response to
1246 Deepwater Horizon oil spill. *The ISME journal* **8**, 1464-1475, doi:10.1038/ismej.2013.254
1247 (2014).

bioRxiv preprint doi: https://doi.org/10.1101/097063; this version posted December 29, 2016. The copyright holder for this preprint (which was not certified by peer review) is the author/funder, who has granted bioRxiv a license to display the preprint in perpetuity. It is made available under aCC-BY-NC-ND 4.0 International license.

48 Jindrova, E., Chocova, M., Demnerova, K. & Brenner, V. Bacterial aerobic degradation of benzene, toluene, ethylbenzene and xylene. *Folia microbiologica* **47**, 83-93 (2002).

49 Pelletier, D. A. & Harwood, C. S. 2-Hydroxycyclohexanecarboxyl coenzyme A dehydrogenase, an enzyme characteristic of the anaerobic benzoate degradation pathway used by Rhodopseudomonas palustris. *Journal of bacteriology* **182**, 2753-2760 (2000).

50 Wood, J. M. Osmosensing by bacteria: signals and membrane-based sensors. *Microbiology and molecular biology reviews : MMBR* **63**, 230-262 (1999).

51 Chow, V., Nong, G. & Preston, J. F. Structure, function, and regulation of the aldouronate utilization gene cluster from Paenibacillus sp. strain JDR-2. *Journal of bacteriology* **189**, 8863-8870, doi:10.1128/JB.01141-07 (2007).

52 Mansilla, M. C., Cybulski, L. E., Albanesi, D. & de Mendoza, D. Control of membrane lipid fluidity by molecular thermosensors. *Journal of bacteriology* **186**, 6681-6688, doi:10.1128/JB.186.20.6681-6688.2004 (2004).

53 Kupferschmied, P., Pechy-Tarr, M., Imperiali, N., Maurhofer, M. & Keel, C. Domain shuffling in a sensor protein contributed to the evolution of insect pathogenicity in plant-beneficial Pseudomonas protegens. *PLoS pathogens* **10**, e1003964, doi:10.1371/journal.ppat.1003964 (2014).

54 Meineke, E. K., Dunn, R. R., Sexton, J. O. & Frank, S. D. Urban warming drives insect pest abundance on street trees. *PloS one* **8**, e59687, doi:10.1371/journal.pone.0059687 (2013).

55 Burland, S. M. & Edwards, E. A. Anaerobic benzene biodegradation linked to nitrate reduction. *Applied and environmental microbiology* **65**, 529-533 (1999).

56 Lieberman, R. L. & Rosenzweig, A. C. Biological methane oxidation: regulation, biochemistry, and active site structure of particulate methane monooxygenase. *Critical reviews in biochemistry and molecular biology* **39**, 147-164, doi:10.1080/10409230490475507 (2004).

57 Wei, J. *et al.* Cysteine biosynthetic enzymes are the pieces of a metabolic energy pump. *Biochemistry* **41**, 8493-8498 (2002).

bioRxiv preprint doi: https://doi.org/10.1101/097063; this version posted December 29, 2016. The copyright holder for this preprint (which was not certified by peer review) is the author/funder, who has granted bioRxiv a license to display the preprint in perpetuity. It is made available under aCC-BY-NC-ND 4.0 International license.

1274 58 Sekowska, A., Kung, H. F. & Danchin, A. Sulfur metabolism in Escherichia coli and related
1275 bacteria: facts and fiction. *Journal of molecular microbiology and biotechnology* **2**, 145-177
1276 (2000).
1277 59 Chakraborty, A. *et al.* Changing bacterial profile of Sundarbans, the world heritage
1278 mangrove: impact of anthropogenic interventions. *World journal of microbiology &*
1279 *biotechnology* **31**, 593-610, doi:10.1007/s11274-015-1814-5 (2015).
1280 60 Elbein, A. D., Pan, Y. T., Pastuszak, I. & Carroll, D. New insights on trehalose: a
1281 multifunctional molecule. *Glycobiology* **13**, 17R-27R, doi:10.1093/glycob/cwg047 (2003).
1282 61 Rojo, F. Degradation of alkanes by bacteria. *Environmental microbiology* **11**, 2477-2490,
1283 doi:10.1111/j.1462-2920.2009.01948.x (2009).
1284 62 Garrett, T. R., Bhakoo, M. & Zhang, Z. B. Bacterial adhesion and biofilms on surfaces. *Prog*
1285 *Nat Sci* **18**, 1049-1056, doi:10.1016/j.pnsc.2008.04.001 (2008).
1286 63 Ullmann, R., Gross, R., Simon, J., Unden, G. & Kroger, A. Transport of C(4)-dicarboxylates in
1287 Wolinella succinogenes. *Journal of bacteriology* **182**, 5757-5764 (2000).
1288 64 Suzuki, K. I. & Hamada, M. Microbacterium. *Bergey's Manual of Systematics of Archaea and*
1289 *Bacteria*, 1-52, doi:10.1002/9781118960608.gbm00104 (2015).
1290 65 Chubiz, L. M., Glekas, G. D. & Rao, C. V. Transcriptional cross talk within the mar-sox-rob
1291 regulon in Escherichia coli is limited to the rob and marRAB operons. *Journal of bacteriology*
1292 **194**, 4867-4875, doi:10.1128/JB.00680-12 (2012).
1293 66 Elsen, S., Swem, L. R., Swem, D. L. & Bauer, C. E. RegB/RegA, a highly conserved redox-
1294 responding global two-component regulatory system. *Microbiology and molecular biology*
1295 *reviews : MMBR* **68**, 263-279, doi:10.1128/MMBR.68.2.263-279.2004 (2004).
1296 67 Lochowska, A. *et al.* Regulation of sulfur assimilation pathways in Burkholderia cenocepacia
1297 through control of genes by the SsuR transcription factor. *Journal of bacteriology* **193**, 1843-
1298 1853, doi:10.1128/JB.00483-10 (2011).

bioRxiv preprint doi: https://doi.org/10.1101/097063; this version posted December 29, 2016. The copyright holder for this preprint (which was not certified by peer review) is the author/funder, who has granted bioRxiv a license to display the preprint in perpetuity. It is made available under aCC-BY-NC-ND 4.0 International license.

68 Yang, S. *et al.* Hydrocarbon degraders establish at the costs of microbial richness, abundance and keystone taxa after crude oil contamination in permafrost environments. *Scientific Reports* **6**, 37473, doi:10.1038/srep37473 (2016).

69 Mori, K., Yamaguchi, K., Sakiyama, Y., Urabe, T. & Suzuki, K. Caldisericum exile gen. nov., sp. nov., an anaerobic, thermophilic, filamentous bacterium of a novel bacterial phylum, Caldiserica phyl. nov., originally called the candidate phylum OP5, and description of Caldisericaceae fam. nov., Caldisericales ord. nov. and Caldisericia classis nov. *International journal of systematic and evolutionary microbiology* **59**, 2894-2898, doi:10.1099/ijs.0.010033-0 (2009).

70 Childers, S. E., Ciufo, S. & Lovley, D. R. Geobacter metallireducens accesses insoluble Fe(III) oxide by chemotaxis. *Nature* **416**, 767-769, doi:10.1038/416767a (2002).

71 Macy, J. M. *et al.* Thauera selenatis gen. nov., sp. nov., a member of the beta subclass of Proteobacteria with a novel type of anaerobic respiration. *International journal of systematic bacteriology* **43**, 135-142, doi:10.1099/00207713-43-1-135 (1993).

72 Daims, H. *et al.* Complete nitrification by Nitrospira bacteria. *Nature* **528**, 504-509, doi:10.1038/nature16461 (2015).

73 Kuever, J. The Family Desulfobulbaceae. *The Prokaryotes: Deltaproteobacteria and Epsilonproteobacteria*, 75-86, doi:10.1007/978-3-642-39044-9_267 (2014).

74 Warren, L. A., Kendra, K. E., Brady, A. L. & Slater, G. F. Sulfur Biogeochemistry of an Oil Sands Composite Tailings Deposit. *Frontiers in microbiology* **6**, 1533, doi:10.3389/fmicb.2015.01533 (2015).

75 Penner, T. J. & Foght, J. M. Mature fine tailings from oil sands processing harbour diverse methanogenic communities. *Canadian journal of microbiology* **56**, 459-470, doi:10.1139/w10-029 (2010).

bioRxiv preprint doi: https://doi.org/10.1101/097063; this version posted December 29, 2016. The copyright holder for this preprint (which was not certified by peer review) is the author/funder, who has granted bioRxiv a license to display the preprint in perpetuity. It is made available under aCC-BY-NC-ND 4.0 International license.

76 Xu, Z., Hansen, M. A., Hansen, L. H., Jacquiod, S. & Sorensen, S. J. Bioinformatic approaches reveal metagenomic characterization of soil microbial community. *PloS one* **9**, e93445, doi:10.1371/journal.pone.0093445 (2014).

77 Barret, M. *et al.* Emergence shapes the structure of the seed microbiota. *Applied and environmental microbiology* **81**, 1257-1266, doi:10.1128/AEM.03722-14 (2015).

78 Bell, T. H. *et al.* Predictable bacterial composition and hydrocarbon degradation in Arctic soils following diesel and nutrient disturbance. *The ISME journal* **7**, 1200-1210, doi:10.1038/ismej.2013.1 (2013).

79 Sun, W. *et al.* Microbial communities inhabiting oil-contaminated soils from two major oilfields in Northern China: Implications for active petroleum-degrading capacity. *Journal of microbiology* **53**, 371-378, doi:10.1007/s12275-015-5023-6 (2015).

Legends

Figure 1. Taxonomic composition of bacterial communities in Noonmati and Barhola oil contaminated soil. Taxonomic cladogram showing all taxa detected at a relative abundance ≥ 0.5% in at least one of the samples. The four rings of the cladogram represent phyla (innermost), class, order and family (outermost) respectively. Circles in the cladogram depict detected taxonomic clades and are colored according to corresponding phyla. Outermost circular rings (external to the cladogram), show rectangular heatmaps depicting abundance of corresponding families in the cladogram. Increasing abundance is represented by increasing opacity.

Figure 2. Taxonomic distribution of bacterial communities in oil contaminated environments. Taxonomic clades detected at an average relative abundance ≥ 2% in at least one of 12 oil contaminated habitats, at the phylum level (A), and at the order level (B).

bioRxiv preprint doi: https://doi.org/10.1101/097063; this version posted December 29, 2016. The copyright holder for this preprint (which was not certified by peer review) is the author/funder, who has granted bioRxiv a license to display the preprint in perpetuity. It is made available under aCC-BY-NC-ND 4.0 International license.

Figure 3. Non-metric multidimensional scaling (NMDS) plot of taxonomic composition of all oil contaminated samples of all habitats. NMDS ordination of 65 oil contaminated samples across 12 habitats was carried out based on Bray-Curtis similarity distances calculated from pairwise taxonomic profile comparisons between all samples. Taxonomic clades present in at least one sample at a relative abundance ≥ 0.5% were used as input. A shorter linear distance between two samples denote greater similarity between the corresponding samples. Samples from 12 environments are depicted by different colors.

Figure 4. Taxonomic biomarkers of bacterial communities from oil polluted habitats. Cladogram showing all taxonomic clades detected at a relative abundance ≥ 0.5% in at least five samples across all habitats. These were used as inputs for LEfSe. Seven rings of the cladogram represent phylum (innermost), class, order, family, genus and species (outermost), respectively. Enlarged circles represent differentially abundant taxa detected as taxonomic biomarkers and are colored corresponding to the individual soil habitat wherein they are over-represented among 12 oil polluted ecosystems (see legend).

Figure 5. Metabolic reconstruction of metagenomes from oil polluted habitats. Cladogram showing KEGG BRITE hierarchical structures denoted by innermost four rings as inferred against detected KEGG metabolic modules for all oil contaminated samples. Outermost ring represents KEGG functional modules that have been detected in at least one of the 65 PICRUSt predicted metagenomes as reconstructed by HUMAnN2. Over-represented metabolic modules inferred by LEfSe are depicted by enlarged circles and are colored corresponding to the oil contaminated habitat they have been identified to be differentially abundant in. Outermost rings (external to the cladogram) depict heat-maps representing significantly or non-significantly present/absent modules across all oil polluted

bioRxiv preprint doi: https://doi.org/10.1101/097063; this version posted December 29, 2016. The copyright holder for this preprint (which was not certified by peer review) is the author/funder, who has granted bioRxiv a license to display the preprint in perpetuity. It is made available under aCC-BY-NC-ND 4.0 International license.

1369 environments. Presence is represented by ≥ 90% coverage and absence by ≤ 10% coverage
1370 of KEGG module as estimated by HUMAnN2. Varied modules are labeled and included in
1371 legend.

1372 **Figure 6. SparCC network plot of global microbial interactions in individual oil polluted**
1373 **habitats.** Significant bacterial associations captured by SparCC (*p*-value < 0.01) with an
1374 absolute correlation magnitude of ≥ 0.6 are presented. Nodes represent detected
1375 phylotypes (OTU clustered at 97% similarity) involved in either significant co-occurrence
1376 (green edges) or co-exclusion (red edges) relationships. Border coloration depicts taxonomic
1377 affiliation of nodes at the phylum level. Node size is proportional to the connectivity of the
1378 node (both positive and negative relationships).

Table 1. Summary of datasets used in the study. (For additional details, refer to Supplementary data Table S1).

Biome Type	ID	Sequencing Platform	Original ID	Location	Depth of sample collection (cm below surface)	Source material for sequencing	Predominant contaminant/hydrocarbon	Reference
Urban	I1	454 GS Junior	Noonmati_Surface	Guwahati, Assam, India	0-10	*In situ* soil	Crude oil	This study
Urban	I2	455 GS Junior	Noonmati_Deep	Guwahati, Assam, India	20-30	*In situ* soil	Crude oil	This study
Urban	I3	456 GS Junior	Barhola_Surface	Barhola, Assam, India	0-10	*In situ* soil	Crude oil	This study
Urban	I4	457 GS Junior	Barhola_Deep	Barhola, Assam, India	20-30	*In situ* soil	Crude oil	This study
Arctic	A1	Ion Torrent PGM	AH1d1, AH1d2	Axel Heiburg, Nunavut, Canada	0-15	Treated microcosm sediment	Diesel oil	[78]
Arctic	A2	Ion Torrent PGM	AK1d1, AK1d2, AK1d3	Toolik Lake, Alaska, USA	0-15	Treated microcosm sediment	Diesel oil	[78]

Arctic	A3	Ion Torrent PGM	AL1d1, AL1d2, AL1d3	Alert, Nunavut, Canada	0-15	Treated microcosm sediment	Diesel oil	[78]
Arctic	A4	Ion Torrent PGM	AVKd1, AVKd2, AVKd3	Akulivik, Quebec, Canada	0-15	Treated microcosm sediment	Diesel oil	[78]
Arctic	A5	Ion Torrent PGM	BDEd1, BDEd2, BDEd3	Baie Deception, Quebec, Canada	0-15	Treated microcosm sediment	Diesel oil	[78]
Arctic	A6	Ion Torrent PGM	BY1d1, BY1d2, BY1d3	Bylot Island, Nunavut, Canada	0-15	Treated microcosm sediment	Diesel oil	[78]
Arctic	A7	Ion Torrent PGM	EBAd1, EBAd2, EBAd3	East Bay, Nunavut, Canada	0-15	Treated microcosm sediment	Diesel oil	[78]
Arctic	A8	Ion Torrent PGM	IQAd1, IQAd2, IQAd3	Iqaluit, Nunavut, Canada	0-15	Treated microcosm sediment	Diesel oil	[78]
Arctic	A9	Ion Torrent PGM	NORd1, NORd2, NORd3	Tromso, Norway	0-15	Treated microcosm sediment	Diesel oil	[78]
Arctic	A10	Ion Torrent PGM	RANd1, RANd2, RANd3	Rankin Inlet, Nunavut, Canada	0-15	Treated microcosm sediment	Diesel oil	[78]
Arctic	A11	Ion Torrent PGM	RUSd1, RUSd2, RUSd3	Yamal, Russia	0-15	Treated microcosm sediment	Diesel oil	[78]

Arctic	A12	Ion Torrent PGM	THUd1, THUd2, THUd3	Thule, Greenland	0-15	Treated microcosm sediment	Diesel oil	[78]
Urban	C1	Illumina Miseq	CQM1	Changqing, China	2-10	*In situ* soil	Crude oil	[79]
Urban	C2	Illumina Miseq	CQM2	Changqing, China	2-10	*In situ* soil	Crude oil	[79]
Urban	C3	Illumina Miseq	CQM3	Changqing, China	2-10	*In situ* soil	Crude oil	[79]
Urban	C4	Illumina Miseq	DQM3	Daqing, China	2-10	*In situ* soil	Crude oil	[79]
Urban	C5	Illumina Miseq	DQM4	Daqing, China	2-10	*In situ* soil	Crude oil	[79]
Urban	C6	Illumina Miseq	DQM5	Daqing, China	2-10	*In situ* soil	Crude oil	[79]
Urban	C7	Illumina Miseq	DQM12	Daqing, China	2-10	*In situ* soil	Crude oil	[79]
Urban	C8	Illumina Miseq	DQM50	Daqing, China	2-10	*In situ* soil	Crude oil	[79]
Urban	C9	Illumina Miseq	DQM200	Daqing, China	2-10	*In situ* soil	Crude oil	[79]
Mangrove	M1	454 GS FLX	T23 2% I, T23 2% II	Restinga da Marambaia, Rio de Janeiro, Brazil	0-20	Treated microcosm sediment	Crude oil	[43]
Mangrove	M2	455 GS FLX	T66 2% I, T66 2% II	Restinga da Marambaia, Rio de	0-20	Treated microcosm sediment	Crude oil	[43]

				Janeiro, Brazil				
Mangrove	M3	456 GS FLX	T23 5% I, T23 5% II	Restinga da Marambaia, Rio de Janeiro, Brazil	0-20	Treated microcosm sediment	Crude oil	[43]
Marine sediment	DWH1	Illumina	SE-20101001-GY-LBNL1-BC-120	Gulf of Mexico	0-1[#]	*In situ* soil	Crude oil	[47]
Marine sediment	DWH2	Illumina	SE-20101001-GY-ALTNF001-BC-139	Gulf of Mexico	0-1[#]	*In situ* soil	Crude oil	[47]
Marine sediment	DWH3	Illumina	SE-20101001-GY-NF006MOD-BC-143	Gulf of Mexico	0-1[#]	*In situ* soil	Crude oil	[47]
Marine sediment	DWH4	Illumina	SE-20101017-GY-D031S-BC-278	Gulf of Mexico	0-1[#]	*In situ* soil	Crude oil	[47]
Marine sediment	DWH5	Illumina	SE-20101017-GY-D040S-BC-315	Gulf of Mexico	0-1[#]	*In situ* soil	Crude oil	[47]
Marine sediment	DWH6	Illumina	SE-20101017-GY-D038SW-BC-331	Gulf of Mexico	0-1[#]	*In situ* soil	Crude oil	[47]
Marine sediment	DWH7	Illumina	SE-20101017-GY-D042S-BC-350	Gulf of Mexico	0-1[#]	*In situ* soil	Crude oil	[47]
Taiga	Tu1	456 GS FLX	1330	Walagan, China	20-30	Treated microcosm sediment	Crude oil	[18]
Taiga	Tu2	456 GS FLX	2330	Walagan North, China	20-30	Treated microcosm sediment	Crude oil	[18]

Taiga	Tu3	456 GS FLX	3330	Taiyuan, China	20-30	Treated microcosm sediment	Crude oil	[18]
Taiga	Tu4	456 GS FLX	4330	Jiagedaqi, China	20-30	Treated microcosm sediment	Crude oil	[18]
Taiga	Tb1	456 GS FLX	1530	Walagan, China	70-80	Treated microcosm sediment	Crude oil	[18]
Taiga	Tb2	456 GS FLX	2530	Walagan North, China	70-80	Treated microcosm sediment	Crude oil	[18]
Taiga	Tb3	456 GS FLX	3530	Taiyuan, China	70-80	Treated microcosm sediment	Crude oil	[18]
Taiga	Tb4	456 GS FLX	4530	Jiagedaqi, China	70-80	Treated microcosm sediment	Crude oil	[18]
Taiga	Tp1	456 GS FLX	1630	Walagan, China	140-150	Treated microcosm sediment	Crude oil	[18]
Taiga	Tp2	456 GS FLX	2630	Walagan North, China	140-150	Treated microcosm sediment	Crude oil	[18]
Taiga	Tp3	456 GS FLX	3630	Taiyuan, China	140-150	Treated microcosm sediment	Crude oil	[18]
Taiga	Tp4	456 GS FLX	4630	Jiagedaqi, China	140-150	Treated microcosm sediment	Crude oil	[18]

Arctic	OSC1	456 GS FLX	2010Suncor Oil Sands Core Run 11 Subsample 1	Alberta, Canada	2,985-2,990	*In situ* soil	Oil sands bitumen	[17]
Arctic	OSC3	456 GS FLX	2010Suncor Oil Sands Core Run 11 Subsample 3	Alberta, Canada	2,985-2,990	*In situ* soil	Oil sands bitumen	[17]
Arctic	OSC4	456 GS FLX	2010Suncor Oil Sands Core Run 11 Subsample 4	Alberta, Canada	2,985-2,990	*In situ* soil	Oil sands bitumen	[17]
Arctic	OSC5	456 GS FLX	2010Suncor Oil Sands Core Run 11 Subsample 5	Alberta, Canada	2,985-2,990	*In situ* soil	Oil sands bitumen	[17]
Arctic	OSC7	456 GS FLX	2010Suncor Oil Sands Core Run 11 Subsample 7	Alberta, Canada	2,985-2,990	*In situ* soil	Oil sands bitumen	[17]
Arctic	OSC9	456 GS FLX	2010Suncor Oil Sands Core Run 11 Subsample 9	Alberta, Canada	2,985-2,990	*In situ* soil	Oil sands bitumen	[17]
Arctic	OSC12	456 GS FLX	2010Suncor Oil Sands Core Run 11 Subsample 13	Alberta, Canada	2,985-2,990	*In situ* soil	Oil sands bitumen	[17]
Arctic	OSTPu1	456 GS FLX	2009Suncor Tailings Pond 5 (6.5 ft)	Alberta, Canada	200	*In situ* soil	Oil sands bitumen	[17]
Arctic	OSTPu2	456 GS FLX	2009Suncor Tailings Pond 5 (8.0 ft)	Alberta, Canada	240	*In situ* soil	Bitumen and various other hydrocarbons	[17]
Arctic	OSTPu3	456 GS FLX	2010Syncrude Tailings Pond MLSB M MFT - 1m	Alberta, Canada	100	*In situ* soil	Bitumen and various other hydrocarbons	[17]

Arctic	OSTPu4	456 GS FLX	2010Syncrude Tailings Pond MLSB N MFT - 1.1m	Alberta, Canada	110	*In situ* soil	Bitumen and various other hydrocarbons	[17]
Arctic	OSTPm2	456 GS FLX	2009Suncor Tailings Pond 5 (25 ft)	Alberta, Canada	750	*In situ* soil	Bitumen and various other hydrocarbons	[17]
Arctic	OSTPm4	456 GS FLX	011Suncor Tailings Pond 6 (7 m)	Alberta, Canada	700	*In situ* soil	Bitumen and various other hydrocarbons	[17]
Arctic	OSTPm6	456 GS FLX	2010Syncrude Tailings Pond MLSB N MFT - 6.1m	Alberta, Canada	610	*In situ* soil	Bitumen and various other hydrocarbons	[17]
Arctic	OSTPd1	456 GS FLX	2009Suncor Tailings Pond 5 (40 ft)	Alberta, Canada	1220	*In situ* soil	Bitumen and various other hydrocarbons	[17]
Arctic	OSTPd2	456 GS FLX	2009SuncorTailings Pond 5 (45 ft)	Alberta, Canada	1370	*In situ* soil	Bitumen and various other hydrocarbons	[17]
Arctic	OSTPd3	456 GS FLX	2010Suncor Tailings Pond 6 (12 m)	Alberta, Canada	1200	*In situ* soil	Bitumen and various other hydrocarbons	[17]
Arctic	OSTPd4	456 GS FLX	2011Suncor Tailings Pond 6 (13 m)	Alberta, Canada	1300	*In situ* soil	Bitumen and various other hydrocarbons	[17]

[#]All samples collected at an average of ~1500 metres below sea level, depth given is from surface of ocean floor marine sediment.

Table 2. Similarities of bacterial community structure within a habitat and between pairs of habitats.

Habitat	India oil refineries	Arctic	China oil refineries	Mangrove	Marine sediments	Taiga upper active layer	Taiga bottom active layer	Taiga permafrost layer	Oil sands core	Oil sands tailings pond upper	Oil sands tailings pond median	Oil sands tailings pond deep
India oil refineries	**0.63 ± 0.06**	0.51 ± 0.07	0.39 ± 0.03	0.44 ± 0.04	0.47 ± 0.04	0.41 ± 0.06	0.41 ± 0.04	0.36 ± 0.05	0.48 ± 0.04	0.46 ± 0.08	0.46 ± 0.08	0.48 ± 0.08
Arctic	0.51 ± 0.07	**0.72 ± 0.07**	0.48 ± 0.05	0.46 ± 0.03	0.42 ± 0.06	0.45 ± 0.07	0.41 ± 0.05	0.39 ± 0.05	0.49 ± 0.05	0.39 ± 0.05	0.39 ± 0.04	0.41 ± 0.06
China oil refineries	0.39 ± 0.03	0.48 ± 0.05	**0.69 ± 0.08**	0.48 ± 0.02	0.40 ± 0.05	0.38 ± 0.06	0.35 ± 0.05	0.34 ± 0.06	0.37 ± 0.06	0.32 ± 0.02	0.35 ± 0.04	0.34 ± 0.05
Mangrove	0.44 ± 0.04	0.46 ± 0.03	0.48 ± 0.02	**0.83 ± 0.02**	0.54 ± 0.05	0.34 ± 0.03	0.34 ± 0.02	0.31 ± 0.02	0.36 ± 0.02	0.41 ± 0.02	0.43 ± 0.04	0.41 ± 0.05
Marine sediments	0.47 ± 0.04	0.42 ± 0.06	0.40 ± 0.05	0.54 ± 0.05	**0.77 ± 0.09**	0.35 ± 0.05	0.35 ± 0.02	0.33 ± 0.05	0.43 ± 0.02	0.38 ± 0.03	0.39 ± 0.03	0.42 ± 0.04
Taiga upper active layer	0.41 ± 0.06	0.45 ± 0.07	0.38 ± 0.06	0.34 ± 0.03	0.35 ± 0.05	**0.52 ± 0.18**	0.59 ± 0.17	0.52 ± 0.18	0.45 ± 0.09	0.34 ± 0.06	0.35 ± 0.05	0.37 ± 0.07
Taiga bottom active layer	0.41 ± 0.04	0.41 ± 0.05	0.35 ± 0.05	0.34 ± 0.02	0.35 ± 0.02	0.59 ± 0.17	**0.57 ± 0.12**	0.55 ± 0.20	0.45 ± 0.05	0.33 ± 0.04	0.34 ± 0.04	0.37 ± 0.06

Taiga permafrost layer	0.36 ± 0.05	0.39 ± 0.05	0.34 ± 0.06	0.31 ± 0.02	0.33 ± 0.05	0.52 ± 0.18	0.55 ± 0.20	**0.45 ± 0.22**	0.42 ± 0.10	0.32 ± 0.06	0.33 ± 0.05	0.36 ± 0.08
Oil sands core	0.48 ± 0.04	0.49 ± 0.05	0.37 ± 0.06	0.36 ± 0.02	0.43 ± 0.02	0.45 ± 0.09	0.45 ± 0.05	0.42 ± 0.10	**0.85 ± 0.09**	0.45 ± 0.05	0.45 ± 0.04	0.56 ± 0.10
Oil sands tailings pond upper	0.46 ± 0.08	0.39 ± 0.05	0.32 ± 0.02	0.41 ± 0.02	0.38 ± 0.03	0.34 ± 0.06	0.33 ± 0.04	0.32 ± 0.06	0.45 ± 0.05	**0.67 ± 0.12**	0.64 ± 0.09	0.63 ± 0.13
Oil sands tailings pond median	0.46 ± 0.08	0.39 ± 0.04	0.35 ± 0.04	0.43 ± 0.04	0.39 ± 0.03	0.35 ± 0.05	0.34 ± 0.04	0.33 ± 0.05	0.45 ± 0.04	0.64 ± 0.09	**0.56 ± 0.05**	0.61 ± 0.12
Oil sands tailings pond deep	0.48 ± 0.08	0.41 ± 0.06	0.34 ± 0.05	0.41 ± 0.05	0.42 ± 0.04	0.37 ± 0.07	0.37 ± 0.06	0.36 ± 0.08	0.56 ± 0.10	0.63 ± 0.13	0.61 ± 0.12	**0.61 ± 0.15**

Table 3: Core modules shared between habitats as detected by HUMAnN2.

Module ID	Definition of modules in KEGG
M00005	PRPP biosynthesis, ribose 5P => PRPP
M00020	Serine biosynthesis, glycerate-3P => serine
M00149	Succinate dehydrogenase, prokaryotes
M00153	Cytochrome d ubiquinol oxidase
M00157	F-type ATPase, prokaryotes and chloroplasts
M00178	Ribosome, bacteria
M00188	NitT/TauT family transport system
M00222	Phosphate transport system
M00223	Phosphonate transport system
M00236	Putative polar amino acid transport system
M00237	Branched-chain amino acid transport system
M00239	Peptides/nickel transport system
M00240	Iron complex transport system
M00250	Lipopolysaccharide transport system
M00254	ABC-2 type transport system
M00255	Lipoprotein-releasing system
M00256	Cell division transport system
M00258	Putative ABC transport system
M00320	Lipopolysaccharide export system

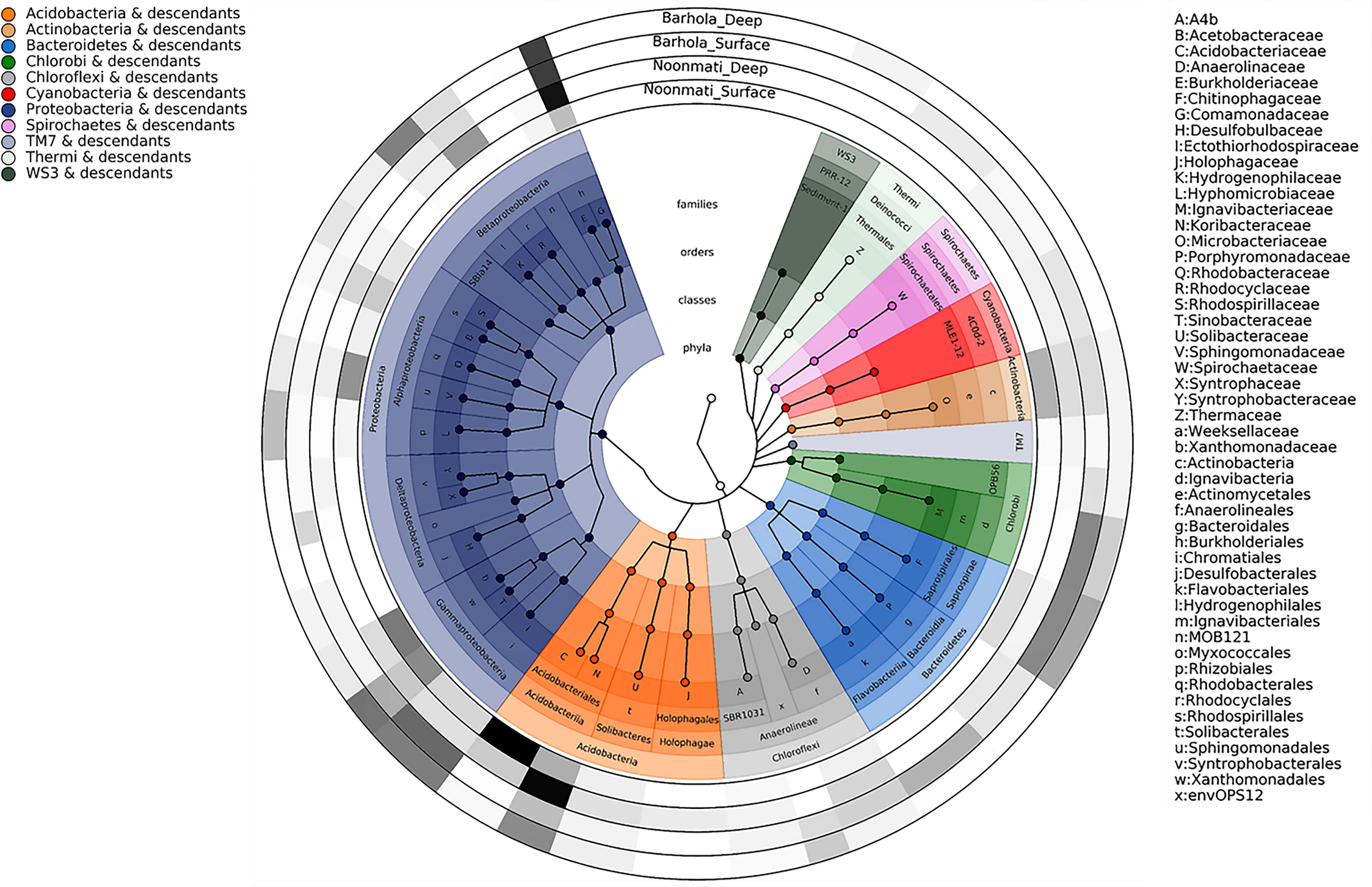
Acidobacteria & descendants
Actinobacteria & descendants
Bacteroidetes & descendants
Chlorobi & descendants
Chloroflexi & descendants
Cyanobacteria & descendants
Proteobacteria & descendants
Spirochaetes & descendants
TM7 & descendants
Thermi & descendants
WS3 & descendants
Barhola_Deep
Barhola_Surface
Noonmati_Deep
Noonmati_Surface
families
orders
classes
phyla
A:A4b
B:Acetobacteraceae
C:Acidobacteriaceae
D:Anaerolinaceae
E:Burkholderiaceae
F:Chitinophagaceae
G:Comamonadaceae
H:Desulfobulbaceae
I:Ectothiorhodospiraceae
J:Holophagaceae
K:Hydrogenophilaceae
L:Hyphomicrobiaceae
M:Ignavibacteriaceae
N:Koribacteraceae
O:Microbacteriaceae
P:Porphyromonadaceae
Q:Rhodobacteraceae
R:Rhodocyclaceae
S:Rhodospirillaceae
T:Sinobacteraceae
U:Solibacteraceae
V:Sphingomonadaceae
W:Spirochaetaceae
X:Syntrophaceae
Y:Syntrophobacteraceae
Z:Thermaceae
a:Weeksellaceae
b:Xanthomonadaceae
c:Actinobacteria
d:Ignavibacteria
e:Actinomycetales
f:Anaerolineales
g:Bacteroidales
h:Burkholderiales
i:Chromatiales
j:Desulfobacterales
k:Flavobacteriales
l:Hydrogenophilales
m:Ignavibacteriales
n:MOB121
o:Myxococcales
p:Rhizobiales
q:Rhodobacterales
r:Rhodocyclales
s:Rhodospirillales
t:Solibacterales
u:Sphingomonadales
v:Syntrophobacterales
w:Xanthomonadales
x:envOPS12

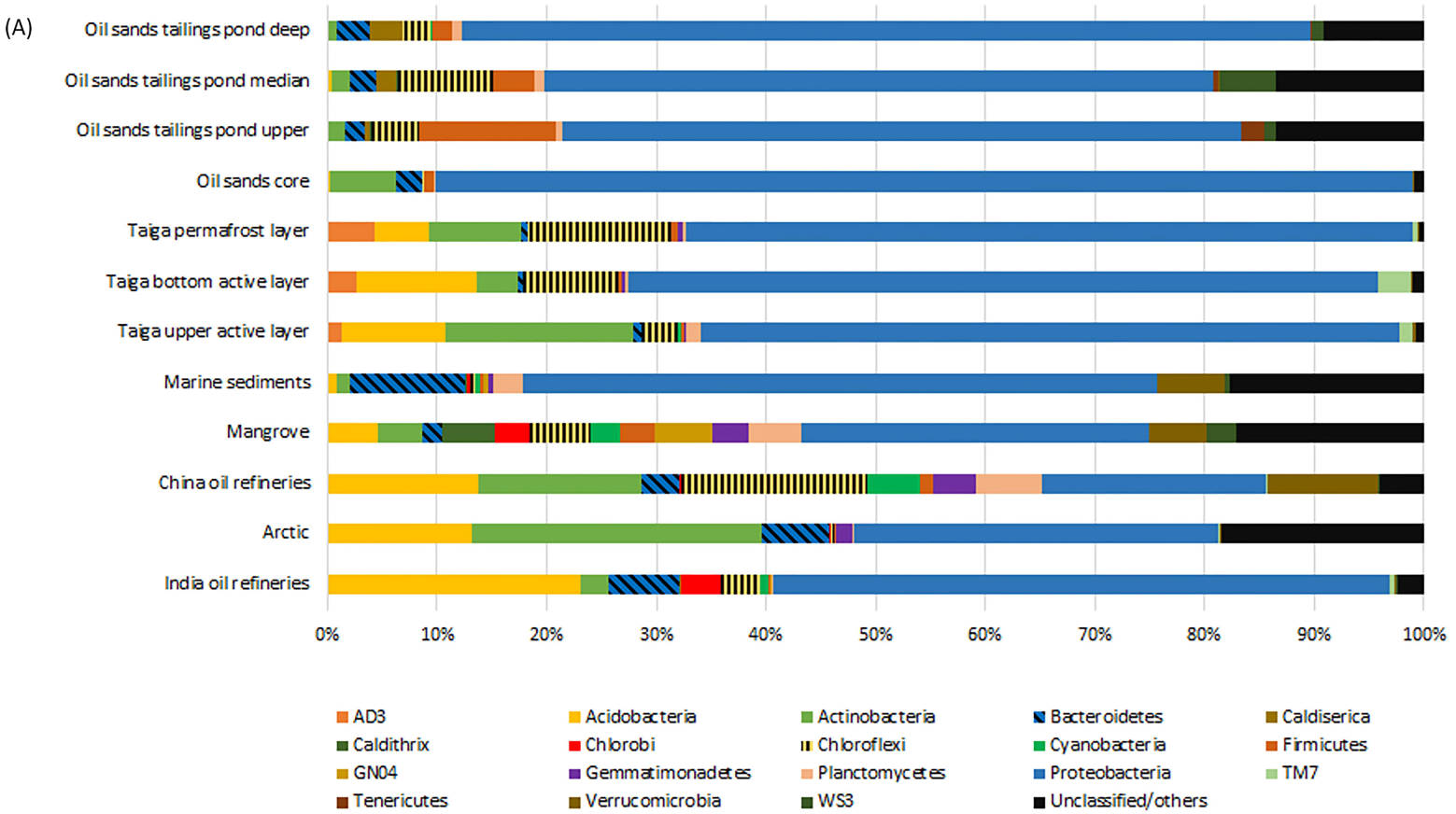
(A)
Oil sands tailings pond deep
Oil sands tailings pond median
Oil sands tailings pond upper
Oil sands core
Taiga permafrost layer
Taiga bottom active layer
Taiga upper active layer
Marine sediments
Mangrove
China oil refineries
Arctic
India oil refineries
0%
10%
20%
30%
40%
50%
60%
70%
80%
90%
100%
AD3
Acidobacteria
Actinobacteria
Bacteroidetes
Caldiserica
Calditrix
Chlorobi
Chloroflexi
Cyanobacteria
Firmicutes
GN04
Gemmatimonadetes
Planctomycetes
Proteobacteria
TM7
Tenericutes
Verrucomicrobia
WS3
Unclassified/others

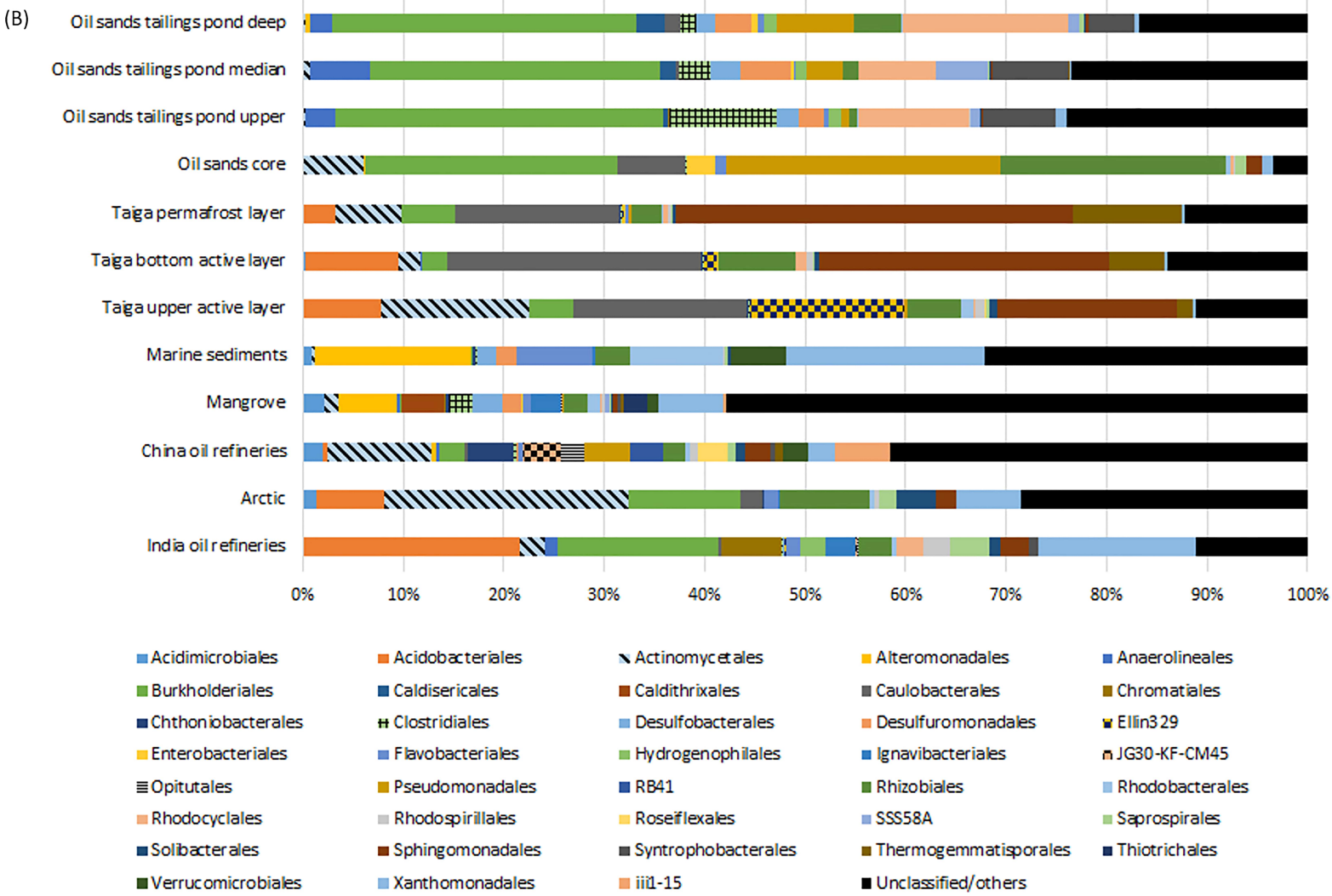
(B)
Oil sands tailings pond deep
Oil sands tailings pond median
Oil sands tailings pond upper
Oil sands core
Taiga permafrost layer
Taiga bottom active layer
Taiga upper active layer
Marine sediments
Mangrove
China oil refineries
Arctic
India oil refineries
0%
10%
20%
30%
40%
50%
60%
70%
80%
90%
100%
Acidimicrobiales
Acidobacteriales
Actinomycetales
Alteromonadales
Anaerolineales
Burkholderiales
Caldisericales
Calditrixales
Caulobacterales
Chromatiales
Chthoniobacterales
Clostridiales
Desulfobacterales
Desulfuromonadales
Ellin329
Enterobacteriales
Flavobacteriales
Hydrogenophilales
Ignavibacteriales
JG30-KF-CM45
Opitutales
Pseudomonadales
RB41
Rhizobiales
Rhodobacterales
Rhodocyclales
Rhodospirillales
Roseiflexales
SSS58A
Saprospirales
Solibacterales
Sphingomonadales
Syntrophobacterales
Thermogemmatisporales
Thiotrichales
Verrucomicrobiales
Xanthomonadales
iii1-15
Unclassified/others

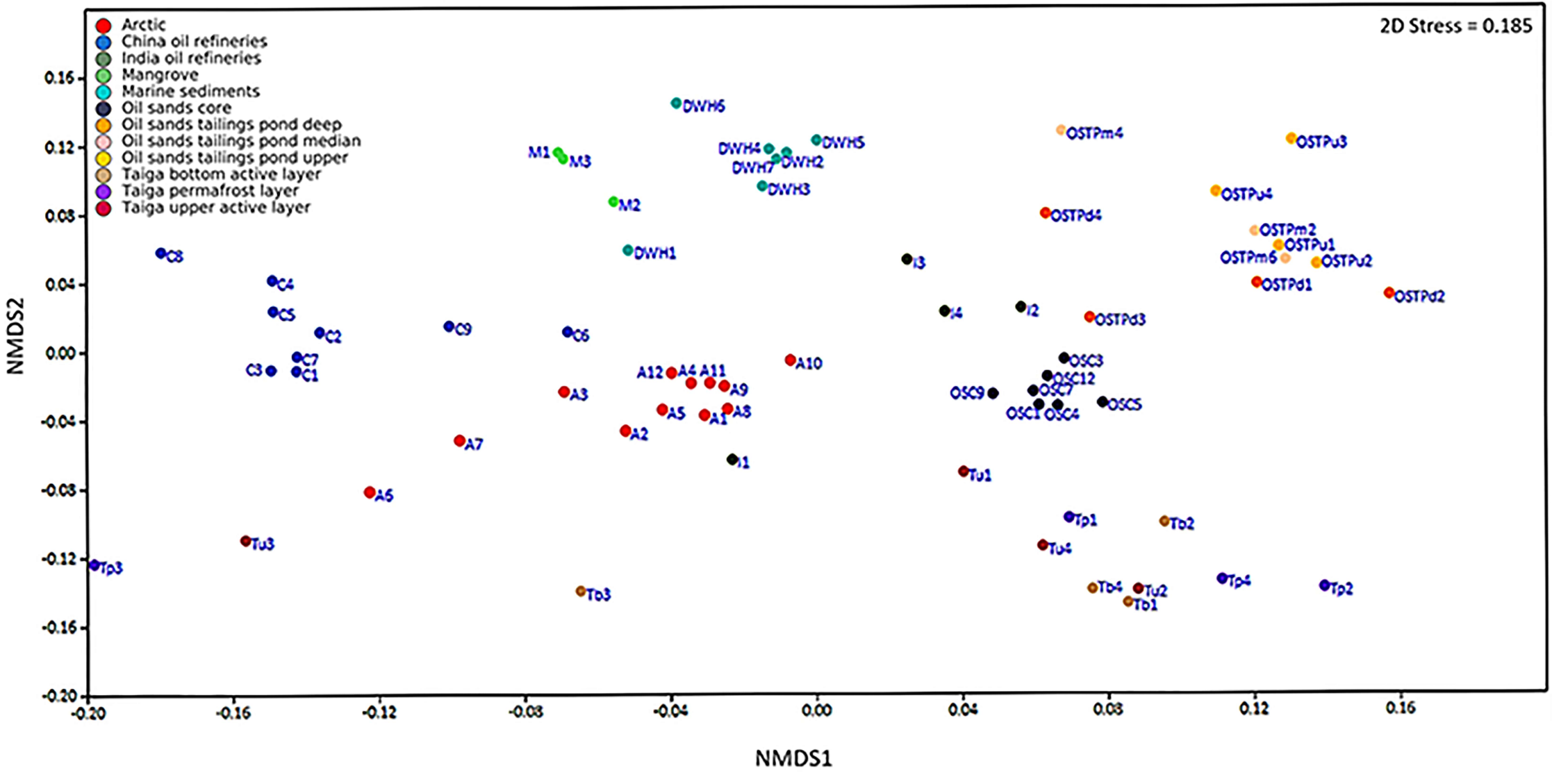

Arctic
China oil refineries
India oil refineries
Mangrove
Marine sediments
Oil sands core
Oil sands tailings pond deep
Oil sands tailings pond median
Oil sands tailings pond upper
Taiga bottom active layer
Taiga permafrost layer
Taiga upper active layer
2D Stress = 0.185
NMDS1
NMDS2
DWH6
DWH5
DWH4
DWH7
DWH2
DWH3
DWH1
M1
M3
M2
OSTPm4
OSTPu3
OSTPu4
OSTPd4
OSTPm2
OSTPu1
OSTPm6
OSTPu2
OSTPd1
OSTPd2
OSTPd3
C8
C4
C5
C2
C7
C3
C1
C9
C6
I3
I4
I2
A10
A12
A4
A11
A9
A3
A5
A1
A8
A2
A7
I1
A6
Tu3
Tp3
Tb3
OSC3
OSC12
OSC9
OSC7
OSC1
OSC4
OSC5
Tu1
Tp1
Tb2
Tu4
Tb4
Tu2
Tb1
Tp4
Tp2

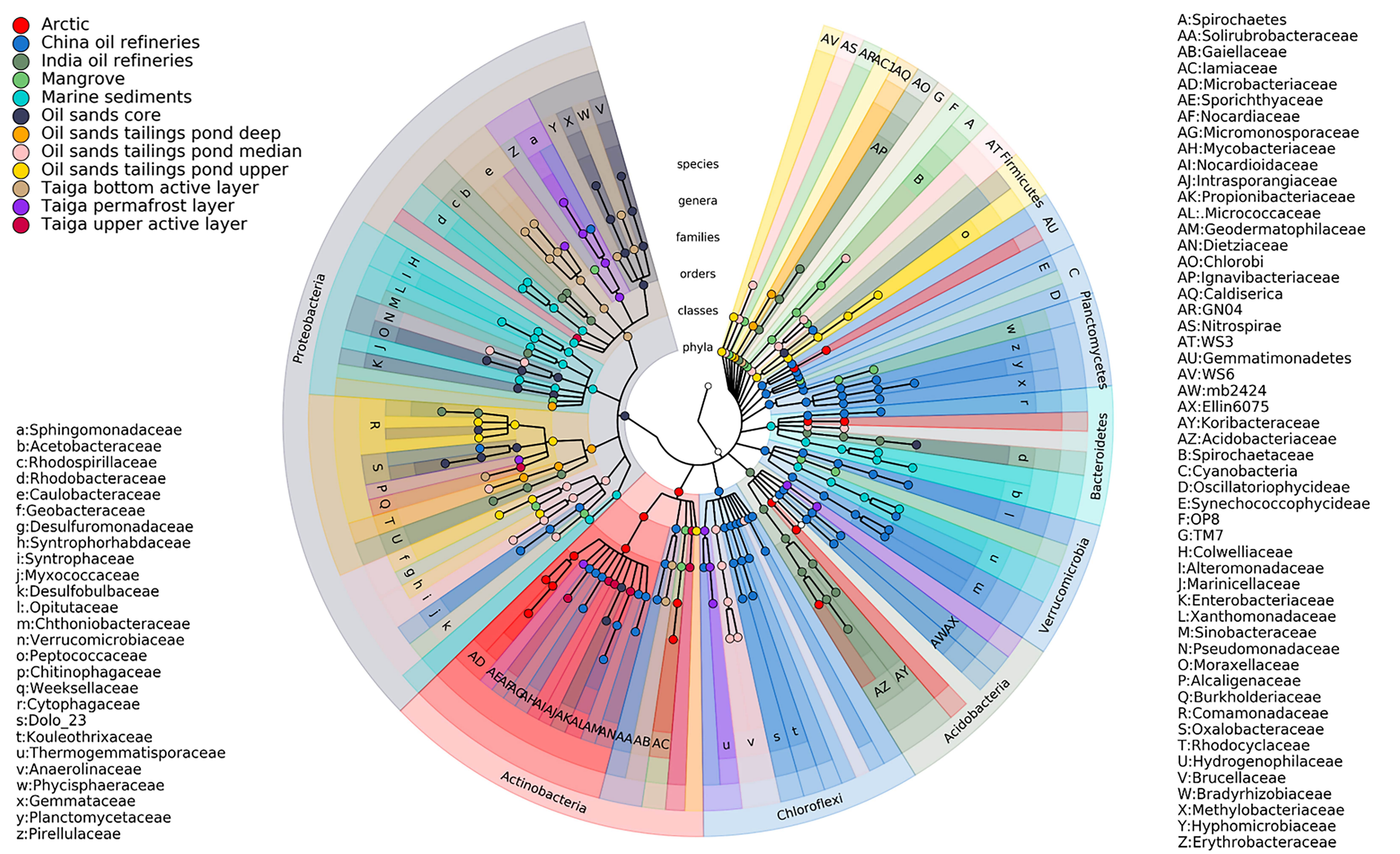
Arctic
China oil refineries
India oil refineries
Mangrove
Marine sediments
Oil sands core
Oil sands tailings pond deep
Oil sands tailings pond median
Oil sands tailings pond upper
Taiga bottom active layer
Taiga permafrost layer
Taiga upper active layer
species
genera
families
orders
classes
phyla
Proteobacteria
Actinobacteria
Chloroflexi
Acidobacteria
Verrucomicrobia
Bacteroidetes
Planctomycetes
Firmicutes
a:Sphingomonadaceae
b:Acetobacteraceae
c:Rhodospirillaceae
d:Rhodobacteraceae
e:Caulobacteraceae
f:Geobacteraceae
g:Desulfuromonadaceae
h:Syntrophorhabdaceae
i:Syntrophaceae
j:Myxococcaceae
k:Desulfobulbaceae
l:.Opitutaceae
m:Chthoniobacteraceae
n:Verrucomicrobiaceae
o:Peptococcaceae
p:Chitinophagaceae
q:Weeksellaceae
r:Cytophagaceae
s:Dolo_23
t:Kouleothrixaceae
u:Thermogemmatisporaceae
v:Anaerolinaceae
w:Phycisphaeraceae
x:Gemmataceae
y:Planctomycetaceae
z:Pirellulaceae
A:Spirochaetes
AA:Solirubrobacteraceae
AB:Gaiellaceae
AC:Iamiaceae
AD:Microbacteriaceae
AE:Sporichthyaceae
AF:Nocardiaceae
AG:Micromonosporaceae
AH:Mycobacteriaceae
AI:Nocardioidaceae
AJ:Intrasporangiaceae
AK:Propionibacteriaceae
AL:.Micrococcaceae
AM:Geodermatophilaceae
AN:Dietziaceae
AO:Chlorobi
AP:Ignavibacteriaceae
AQ:Caldiserica
AR:GN04
AS:Nitrospirae
AT:WS3
AU:Gemmatimonadetes
AV:WS6
AW:mb2424
AX:Ellin6075
AY:Koribacteraceae
AZ:Acidobacteriaceae
B:Spirochaetaceae
C:Cyanobacteria
D:Oscillatoriophycideae
E:Synechococcophycideae
F:OP8
G:TM7
H:Colwelliaceae
I:Alteromonadaceae
J:Marinicellaceae
K:Enterobacteriaceae
L:Xanthomonadaceae
M:Sinobacteraceae
N:Pseudomonadaceae
O:Moraxellaceae
P:Alcaligenaceae
Q:Burkholderiaceae
R:Comamonadaceae
S:Oxalobacteraceae
T:Rhodocyclaceae
U:Hydrogenophilaceae
V:Brucellaceae
W:Bradyrhizobiaceae
X:Methylobacteriaceae
Y:Hyphomicrobiaceae
Z:Erythrobacteraceae

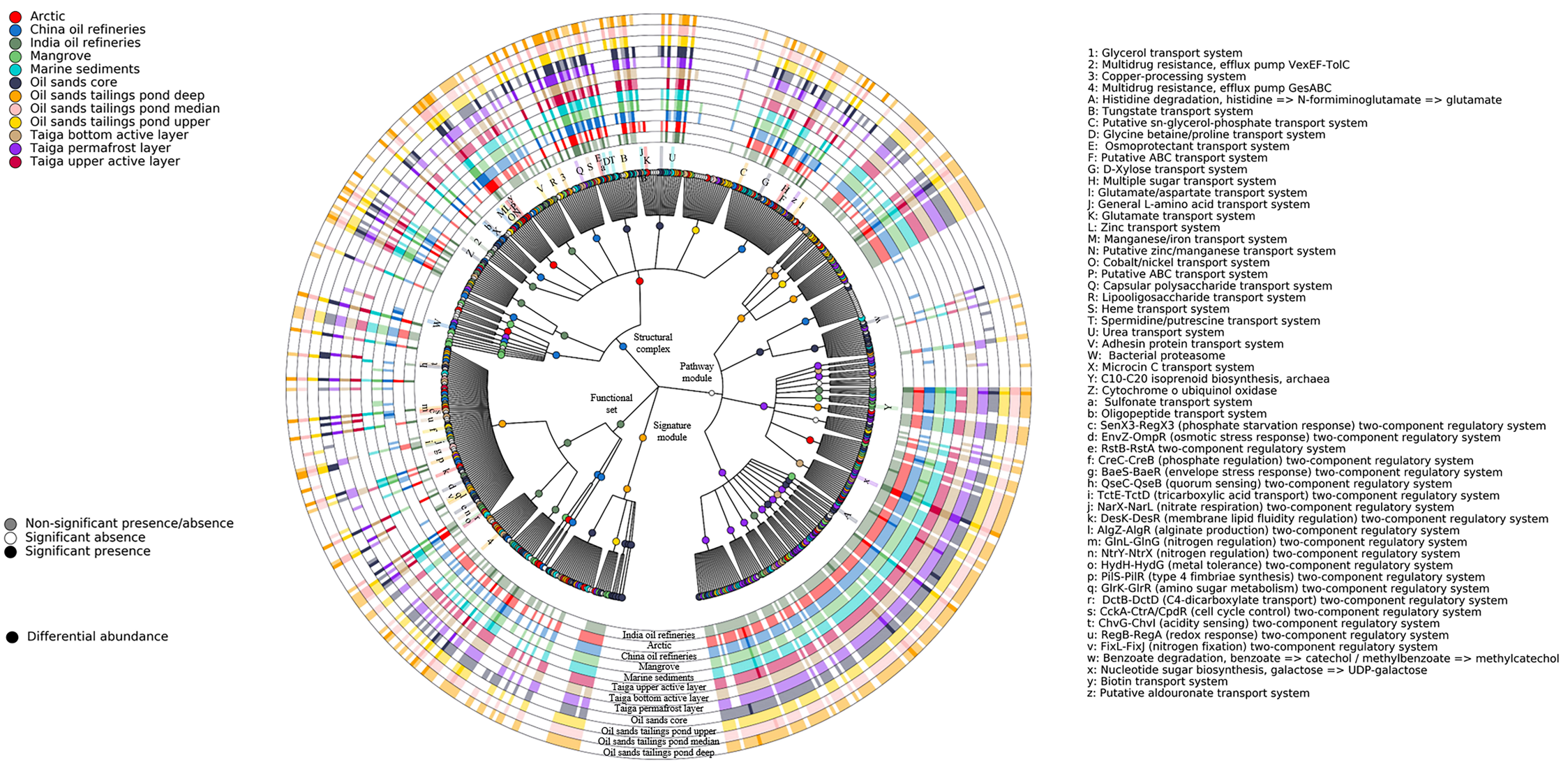
Arctic
China oil refineries
India oil refineries
Mangrove
Marine sediments
Oil sands core
Oil sands tailings pond deep
Oil sands tailings pond median
Oil sands tailings pond upper
Taiga bottom active layer
Taiga permafrost layer
Taiga upper active layer
Non-significant presence/absence
Significant absence
Significant presence
Differential abundance
Structural complex
Pathway module
Functional set
Signature module
India oil refineries
Arctic
China oil refineries
Mangrove
Marine sediments
Taiga upper active layer
Taiga bottom active layer
Taiga permafrost layer
Oil sands core
Oil sands tailings pond upper
Oil sands tailings pond median
Oil sands tailings pond deep
1: Glycerol transport system
2: Multidrug resistance, efflux pump VexEF-TolC
3: Copper-processing system
4: Multidrug resistance, efflux pump GesABC
A: Histidine degradation, histidine => N-formiminoglutamate => glutamate
B: Tungstate transport system
C: Putative sn-glycerol-phosphate transport system
D: Glycine betaine/proline transport system
E: Osmoprotectant transport system
F: Putative ABC transport system
G: D-Xylose transport system
H: Multiple sugar transport system
I: Glutamate/aspartate transport system
J: General L-amino acid transport system
K: Glutamate transport system
L: Zinc transport system
M: Manganese/iron transport system
N: Putative zinc/manganese transport system
O: Cobalt/nickel transport system
P: Putative ABC transport system
Q: Capsular polysaccharide transport system
R: Lipooligosaccharide transport system
S: Heme transport system
T: Spermidine/putrescine transport system
U: Urea transport system
V: Adhesin protein transport system
W: Bacterial proteasome
X: Microcin C transport system
Y: C10-C20 isoprenoid biosynthesis, archaea
Z: Cytochrome o ubiquinol oxidase
a: Sulfonate transport system
b: Oligopeptide transport system
c: SenX3-RegX3 (phosphate starvation response) two-component regulatory system
d: EnvZ-OmpR (osmotic stress response) two-component regulatory system
e: RstB-RstA two-component regulatory system
f: CreC-CreB (phosphate regulation) two-component regulatory system
g: BaeS-BaeR (envelope stress response) two-component regulatory system
h: QseC-QseB (quorum sensing) two-component regulatory system
i: TctE-TctD (tricarboxylic acid transport) two-component regulatory system
j: NarX-NarL (nitrate respiration) two-component regulatory system
k: DesK-DesR (membrane lipid fluidity regulation) two-component regulatory system
l: AlgZ-AlgR (alginate production) two-component regulatory system
m: GlnL-GlnG (nitrogen regulation) two-component regulatory system
n: NtrY-NtrX (nitrogen regulation) two-component regulatory system
o: HydH-HydG (metal tolerance) two-component regulatory system
p: PilS-PilR (type 4 fimbriae synthesis) two-component regulatory system
q: GlrK-GlrR (amino sugar metabolism) two-component regulatory system
r: DctB-DctD (C4-dicarboxylate transport) two-component regulatory system
s: CckA-CtrA/CpdR (cell cycle control) two-component regulatory system
t: ChvG-ChvI (acidity sensing) two-component regulatory system
u: RegB-RegA (redox response) two-component regulatory system
v: FixL-FixJ (nitrogen fixation) two-component regulatory system
w: Benzoate degradation, benzoate => catechol / methylbenzoate => methylcatechol
x: Nucleotide sugar biosynthesis, galactose => UDP-galactose
y: Biotin transport system
z: Putative aldouronate transport system

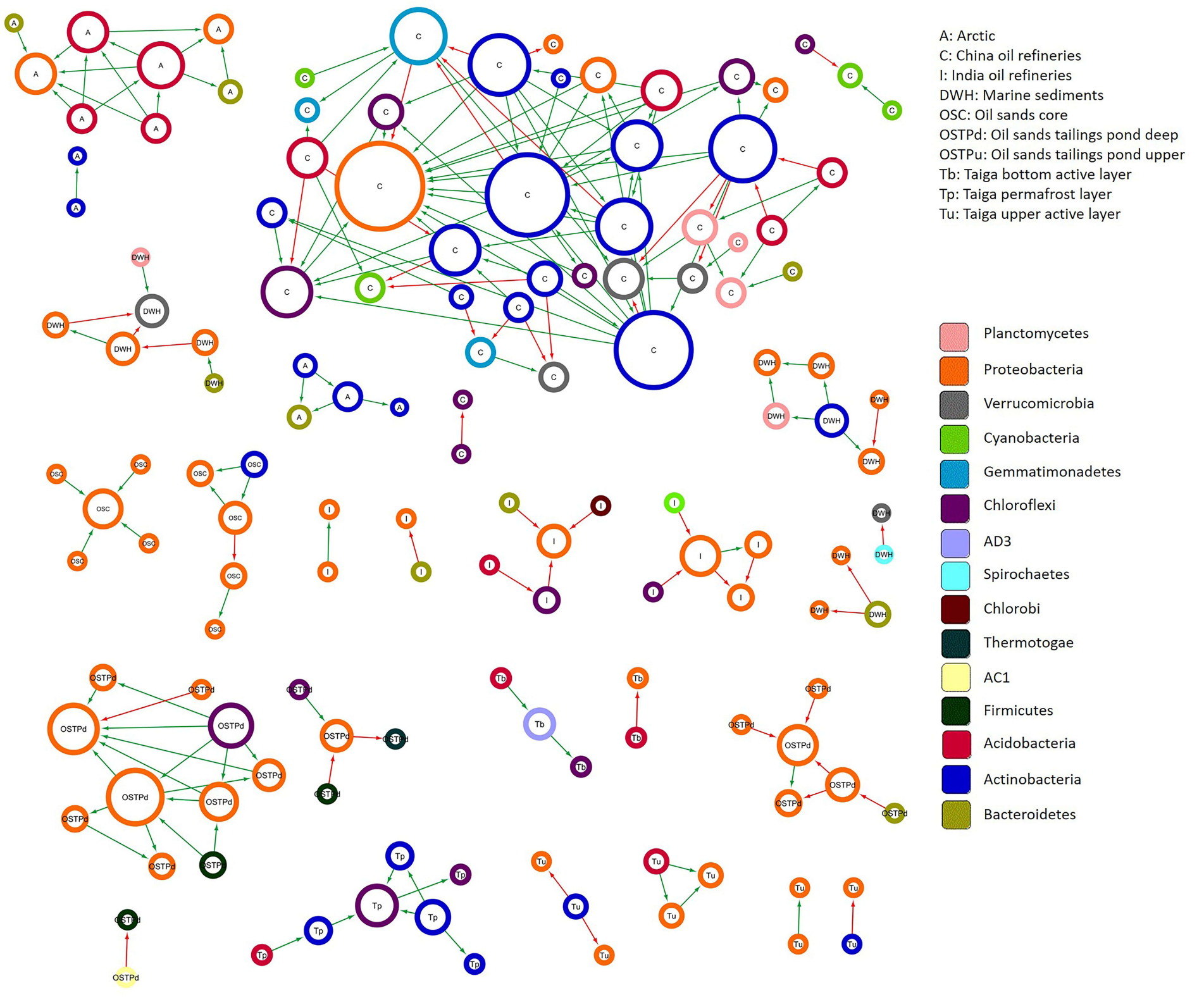
A: Arctic
C: China oil refineries
I: India oil refineries
DWH: Marine sediments
OSC: Oil sands core
OSTPd: Oil sands tailings pond deep
OSTPu: Oil sands tailings pond upper
Tb: Taiga bottom active layer
Tp: Taiga permafrost layer
Tu: Taiga upper active layer
Planctomycetes
Proteobacteria
Verrucomicrobia
Cyanobacteria
Gemmatimonadetes
Chloroflexi
AD3
Spirochaetes
Chlorobi
Thermotogae
AC1
Firmicutes
Acidobacteria
Actinobacteria
Bacteroidetes